REMARKS

Introduction:

Claims 1-6 and 8-25 are pending in the present application. Applicant is amending herewith Claim 1. Following entry of this amendment, Claims 1-6 and 8-25 will still be pending. Applicant submits that these claims are entitled to further examination. Applicant respectfully requests reconsideration of the present application in view of the foregoing amendment and the following remarks.

The Office Action

Claim 1 was objected to as requiring the article "a" be inserted before the word "curved." Claims 1, 2, 5-11, 15, 18-20 and 23-25 was rejected under 35 U.S.C. §103(a) as being obvious and unpatentable over DE 1584006. Applicant respectfully traverses the foregoing rejection. Claims 3, 4, 12-14, 16, 17, 21 and 22 were objected to as being dependent upon a rejected base claim.

Claim Objections

Claim 1 was objected to as requiring the article "a" be inserted before the word "curved." Applicant is amending Claim 1 herewith to insert an "a" before the word "curved" as requested.

Rejection Under 35 U.S.C. § 103

Claims 1, 2, 5-11, 15, 18-20 and 23-25 was rejected under 35 U.S.C. §103(a) as being obvious and unpatentable over DE 1584006. The rejection states that it would have been an obvious matter of design choice to make the different portions of the groove and engagement means of whatever form or shape was desired or expedient. Applicant respectfully disagrees.

It is respectfully submitted that the present rejection is improper for the following two reasons: (i) modifying DE 1584006 as proposed by the Examiner is contrary to the teaching of DE 1584006; and (ii) even if such a modification were made, the resultant combination still does not arrive at the claimed invention.

Proposed Modification is Contrary to Teaching

DE 1584006 discloses a hinge assembly including a pivot pin 13. The pivot pin 13 includes a recess 14 having a first, straight side 18 and a second, chamfered side 16. A ball bearing 21 is biased into engagement with the recess 14, as shown in Figure. 1. In use, the ball bearing 21 resists axial withdrawal of the pivot pin 13 from the hinge assembly. However, the chamfered side 16 is so shaped as to urge the ball bearing 21 out of the recess 14 upon application of a suitable axial withdrawal force to the pivot pin 13. Consequently it is possible to withdraw the pivot pin 13 by applying a desired axial withdrawal force to the pivot pin 13 so as to overcome a threshold force which is defined by the respective geometries of the ball bearing 21 and the chamfered side 16, along with the strength of the bias.

It follows that DE 1584006 is concerned with the provision of a hinge assembly in which it is possible to remove the pivot pin 13 upon application of a suitable axial withdrawal force. This is totally contrary to the present invention wherein the pin is **prevented** from any axial movement (not just removal) by application of an axial force (however great). Accordingly, DE 1584006 is unconcerned with the provision of a hinge assembly in which the pivot pin cannot be removed regardless of the force applied thereto. In other words, modifying DE 1584006 to make the pin axially immovable goes against the

sole purpose of the DE 1584006. Accordingly, a skilled artisan seeing DE 1584006 would not seek to modify it to make the pivot pin immovable.

It follows that the skilled artisan could not use the teaching of DE 1584006 as a starting point for arriving at the present invention because DE 1584006 requires axial movement of the pivot pin 13 to initiate disengagement of the retaining means. Thus, the modification suggested by the Examiner is contrary to the teaching of DE 1584006. Therefore, such modification would not be obvious to a skilled artisan. Accordingly, rejection of Claims 1, 2, 5-11, 15, 18-20 and 23-25 under 35 U.S.C. §103 is improper and should be withdrawn.

(ii) Resultant Combination Does Not Arrive at the Invention

Even if the skilled worker were to combine the teaching of DE 1584006 with either of the patent to Hansen et al. (U.S. Patent No. 3,796,464) or the patent to Kramer (U.S. Patent No. 5,452,501), he would not arrive at the presently claimed invention.

The patent to Hansen et al. discloses an arrangement in which a keeper 26 has a protuberance 30 which is received in a groove 12. Lines 5 to 8 of column 2 of Hansen et al. mention that the keeper 26 is preferably made of compressible material; *e.g.*, rubber or plastic, or otherwise constructed so that the protuberance 30 can be depressed from groove. Accordingly, Hansen et al. teaches that upon application of a suitable axial withdrawal force to the bit 10 the protuberance 30 deforms thereby allowing removal of the bit 10.

Therefore, both DE 1584006 and Hansen et al. teach the skilled artisan that application of a suitable axial withdrawal force permits withdrawal of the desired pivot pin/bit. Consequently, a combination of DE 1584006 and Hansen et al. does not disclose or

suggest an arrangement which prevents axial withdrawal of a pivot pin, regardless of the axial force applied thereto.

It follows that the presently claimed invention is not obvious to a skilled artisan based on a combination of DE 1584006 and Hansen et al.

The patent to Kramer describes a hinge arrangement for checking the door of a motor vehicle when in the open position. Figure 6 shows a strap 14 which is pivotally mounted in a base 12. The strap includes a pair of ball bearings 60, 68 each of which cooperates with a corresponding check profile cam surface 34, 36 to restrain the strap in one of two positions. When moving the strap 14 relative to the base 12, the ball bearings 60, 68 roll across the flat opposed surfaces of the flanges 26, 28 until they reach a first lobe 37 in the check profile 34, 36. The first lobe 37 establishes the first check position of the strap as an axial spring 64 urges the ball bearings 60, 68 to be seated in the lobe 37. Line 61 of column 6 to line 1 of column 7 of Kramer mention that further rotation of the strap 14 pushes the ball bearings 60, 68 inwards against the spring force so that they are able to roll out of the lobe 37 defining the first check position. The ball bearings 60, 68 are then able to enter a second lobe 39 which defines a second check position.

Accordingly, Kramer teaches that application of a sufficient force to the strap 14 causes the engaging means; *i.e.*, the ball bearings 60, 68, to move, thereby allowing further movement of the strap 14. Therefore, Kramer teaches that the application of a suitable force to a member which it is desired to move permits movement of the said member. Consequently, the skilled artisan in combining DE 1584006 and Kramer could not arrive at an arrangement which prevents axial withdrawal; *i.e.*, movement of a pivot pin, regardless of the axial force applied thereto.

It follows that the presently claimed invention is not obvious to a skilled artisan based on a combination of DE 1584006 and Kramer. The present invention is not a matter of mere design choice, as alleged by the Examiner, but, rather, produces a different result not taught or suggested by the prior art.

In view of the foregoing, it is respectfully submitted that Claims 1, 2, 5-11, 15, 18-20 and 23-25 are not obvious in view of DE 1584006, Kramer and Hansem et al. Accordingly, withdrawal of the rejection of Claims 1, 2, 5-11, 15, 18-20 and 23-25 under 35 U.S.C. §103(a) is respectfully requested.

Conclusion

Applicant respectfully requests reconsideration of the present application in view of the foregoing amendment and remarks. Such action is courteously solicited. Applicant further requests that the Examiner call the undersigned attorney if allowance of the claims can be facilitated by examiner's amendment, telephone interview or otherwise.

Respectfully submitted,

By: Robert E. Richards
Reg. No. 29,105

KILPATRICK STOCKTON LLP
1100 Peachtree Street, Suite 2800
Atlanta, Georgia 30309
Tel: (404) 815-6500
Fax: (404) 815-6555
Our Docket: 43191-270021

THE ROCK PHYSICS HANDBOOK

TOOLS FOR SEISMIC ANALYSIS IN POROUS MEDIA

Gary Mavko
Stanford University

Tapan Mukerji
Stanford University

Jack Dvorkin
Stanford University

CAMBRIDGE
UNIVERSITY PRESS

CONTENTS

PART 4

EFFECTIVE MEDIA

4.1 HASHIN–SHTRIKMAN BOUNDS

SYNOPSIS

If we wish to predict the effective elastic moduli of a mixture of grains and pores theoretically, we generally need to specify (1) the volume fractions of the various phases, (2) the elastic moduli of the various phases, and (3) the geometric details of how the phases are arranged relative to each other. If we specify only the volume fractions and the constituent moduli, the best we can do is to predict the upper and lower bounds (shown shematically in Figure 4.1.1).

At any given volume fraction of constituents the effective modulus will fall between the bounds (somewhere along the vertical dashed line in the plot of bulk modulus, Figure 4.1.1), but its precise value depends on the geometric details. We use, for example, terms like "stiff pore shapes" and "soft pore shapes." Stiffer shapes cause the value to be higher within the allowable range; softer shapes cause the value to be lower. The best bounds, defined as giving the narrowest possible range without specifying anything about the geometries of the constituents, are the Hashin–Shtrikman bounds (Hashin and Shtrikman, 1963), given by

$$K^{\mathrm{HS}\pm} = K_1 + \frac{f_2}{(K_2 - K_1)^{-1} + f_1\left(K_1 + \frac{4}{3}\mu_1\right)^{-1}}$$

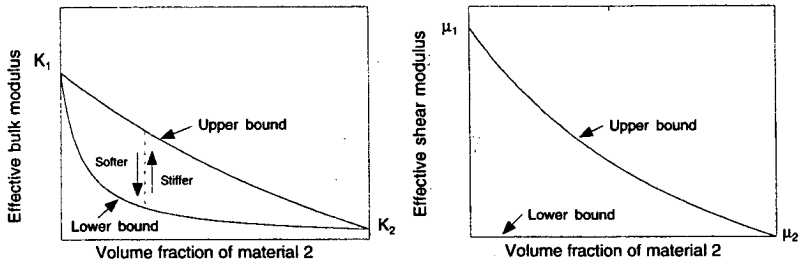

Figure 4.1.1. Schematic representation of the upper and lower bounds on the elastic bulk and shear moduli.

$$\mu^{\mathrm{HS}\pm} = \mu_1 + \frac{f_2}{(\mu_2 - \mu_1)^{-1} + \frac{2f_1(K_1+2\mu_1)}{5\mu_1(K_1+\frac{4}{3}\mu_1)}}$$

where

K_1, K_2 = bulk moduli of individual phases
μ_1, μ_2 = shear moduli of individual phases
f_1, f_2 = volume fractions of individual phases

Upper and lower bounds are computed by interchanging which material is termed 1 and which is termed 2. Generally, the expressions give the upper bound when the stiffest material is termed 1 in the expressions above, and the lower bound when the softest material is termed 1.

The physical interpretation of the bounds for bulk modulus is shown schematically in Figure 4.1.2. The space is filled by an assembly of spheres of material 2, each surrounded by a shell of material 1. Each sphere and its shell has precisely the volume fractions f_1 and f_2. The upper bound is realized when the stiffer material forms the shell; the lower bound is realized when it is in the core.

A more general form of the bounds, which can be applied to more than two phases (Berryman, 1995), can be written as

$$K^{\mathrm{HS}+} = \Lambda(\mu_{\max}), \quad K^{\mathrm{HS}-} = \Lambda(\mu_{\min})$$
$$\mu^{\mathrm{HS}+} = \Gamma(\zeta(K_{\max}, \mu_{\max})), \quad \mu^{\mathrm{HS}-} = \Gamma(\zeta(K_{\min}, \mu_{\min}))$$

where

$$\Lambda(z) = \left\langle \frac{1}{K(r) + \frac{4}{3}z} \right\rangle^{-1} - \frac{4}{3}z$$

$$\Gamma(z) = \left\langle \frac{1}{\mu(r) + z} \right\rangle^{-1} - z$$

$$\zeta(K, \mu) = \frac{\mu}{6}\left(\frac{9K + 8\mu}{K + 2\mu}\right)$$

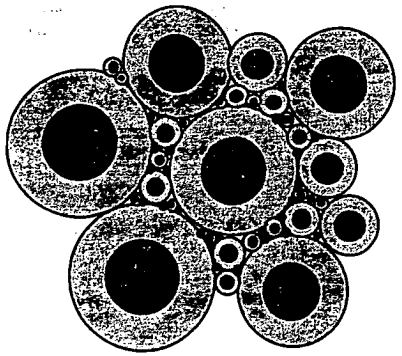

Figure 4.1.2. Physical interpretation of the Hashin–Shtrikman bounds for bulk modulus of a two-phase material.

The brackets $\langle\cdot\rangle$ indicate an average over the medium, which is the same as an average over the constituents weighted by their volume fractions.

EXAMPLE

Compute the Hashin–Shtrikman upper and lower bounds on the bulk and shear moduli for a mixture of quartz, calcite, and water. The porosity (water fraction) is 27 percent; quartz is 80 percent by volume of the solid fraction, and calcite is 20 percent by volume of the solid fraction. The moduli of the individual constituents are

$$K_{\text{quartz}} = 36\,\text{GPa}, \quad K_{\text{calcite}} = 75\,\text{GPa}, \quad K_{\text{water}} = 2.2\,\text{GPa},$$

$$\mu_{\text{quartz}} = 45\,\text{GPa}, \quad \mu_{\text{calcite}} = 31\,\text{GPa}, \quad \text{and} \quad \mu_{\text{water}} = 0\,\text{GPa}.$$

Hence

$$\mu_{\min} = 0\,\text{GPa}, \quad \mu_{\max} = 45\,\text{GPa}, \quad K_{\min} = 2.2\,\text{GPa}, \quad \text{and} \quad K_{\max} = 75\,\text{GPa}.$$

$$K^{\text{HS}-} = \Lambda(\mu_{\min})$$

$$= \left[\frac{\phi}{2.2} + \frac{(1-\phi)(0.8)}{36.0} + \frac{(1-\phi)(0.2)}{75.0}\right]^{-1} - \frac{4}{3}(0)$$

$$= 7.10\,\text{GPa}$$

$$K^{\text{HS}+} = \Lambda(\mu_{\max})$$

$$= \left[\frac{\phi}{2.2 + \left(\frac{4}{3}\right)45} + \frac{(1-\phi)(0.8)}{36.0 + \left(\frac{4}{3}\right)45} + \frac{(1-\phi)(0.2)}{75.0 + \left(\frac{4}{3}\right)45.0}\right]^{-1} - \left(\frac{4}{3}\right)45$$

$$= 26.9\,\text{GPa}$$

$$\zeta(K_{\max}, \mu_{\max}) = \frac{45}{6}\left(\frac{9\times 75 + 8\times 45}{75 + 2\times 45}\right) = 47.0\,\text{GPa}$$

$$\zeta(K_{\min}, \mu_{\min}) = 0\,\text{GPa}$$

$$\mu^{\text{HS}+} = \Gamma(\zeta(K_{\max}, \mu_{\max}))$$

$$= \left[\frac{\phi}{47.0} + \frac{(1-\phi)(0.8)}{45.0 + 47.0} + \frac{(1-\phi)(0.2)}{31.0 + 47.0}\right]^{-1} - 47.0$$

$$= 24.6\,\text{GPa}$$

$$\mu^{\text{HS}-} = \Gamma(\zeta(K_{\min}, \mu_{\min}))$$

$$= 0$$

The separation between the upper and lower bounds depends on how different the constituents are. As shown in Figure 4.1.3, the bounds are often quite similar when mixing solids, for the moduli of common minerals are usually within a factor of two of each other. Because many effective medium models (e.g., Biot, Gassmann, Kuster–Toksöz, etc.) assume a homogeneous mineral modulus, it is often useful (and adequate) to represent a mixed mineralogy with an "average mineral" equal to either one of the bounds or to their average $(M^{\text{HS}+} + M^{\text{HS}-})/2$. On the other hand, when the constituents are quite different (such as minerals and pore fluids), the bounds become quite separated, and we lose some of the predictive value.

Note that when $\mu_{\min} = 0$, $K^{\text{HS}-}$ is the same as the Reuss bound. In this case, the Reuss or Hashin–Shtrikman lower bound describes the moduli of a suspension of grains in a pore fluid exactly (see Section 4.2 on Voigt–Reuss bounds and also Section 4.3 on Wood's relation). These also describe the moduli of a mixture of fluids or gases, or both.

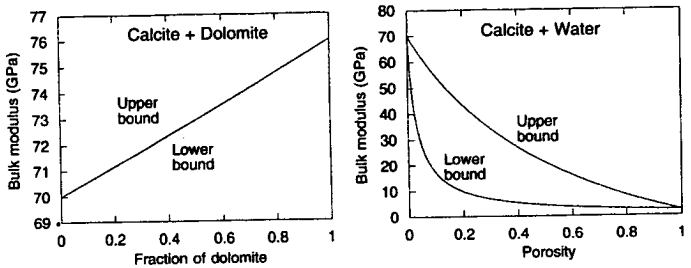

Figure 4.1.3

When all phases have the same shear modulus, $\mu = \mu_{min} = \mu_{max}$, the upper and lower bounds become identical and we get the expression by Hill (1963) for the effective bulk modulus of a composite with uniform shear modulus (see Section 4.5 on composites with uniform shear modulus).

USES

The bounds described in this section can be used for the following:

- To compute the estimated range of average mineral modulus for a mixture of mineral grains.
- To compute the upper and lower bounds for a mixture of mineral and pore fluid.

ASSUMPTIONS AND LIMITATIONS

The bounds described in this section apply under the following conditions:

- Each constituent is isotropic, linear, elastic.
- The rock is isotropic linear elastic.

4.2 VOIGT AND REUSS BOUNDS

SYNOPSIS

If we wish to predict the effective elastic moduli of a mixture of grains and pores theoretically, we generally need to specify (1) the volume fractions of the various phases, (2) the elastic moduli of the various phases, and (3) the geometric details of how the phases are arranged relative to each other. If we specify only the volume fractions and the constituent moduli, the best we can do is to predict the upper and lower bounds (shown schematically in Figure 4.2.1).

At any given volume fraction of constituents, the effective modulus will fall between the bounds (somewhere along the vertical dashed line in Figure 4.2.1), but its precise value depends on the geometric details. We use, for example, terms like "stiff pore shapes" and "soft pore shapes." Stiffer shapes cause the value to be higher within the allowable range; softer shapes cause the value to be lower. The simplest, but not necessarily the best, bounds are the Voigt and Reuss bounds. (See also Section 4.1 on Hashin–Shtrikman bounds, which are narrower.)

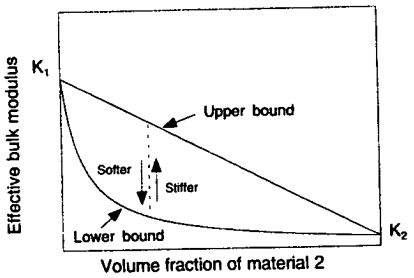

Figure 4.2.1

The **Voigt upper bound** of the effective elastic modulus, M_V, of N phases is

$$M_V = \sum_{i=1}^{N} f_i M_i$$

where

f_i = the volume fraction of the ith medium
M_i = the elastic modulus of the ith medium

The Voigt bound is sometimes called the **isostrain average** because it gives the ratio of average stress to average strain when all constituents are assumed to have the same strain.

The **Reuss lower bound** of the effective elastic modulus, M_R, is (Reuss, 1929)

$$\frac{1}{M_R} = \sum_{i=1}^{N} \frac{f_i}{M_i}$$

The Reuss bound is sometimes called the **isostress average** because it gives the ratio of average stress to average strain when all constituents are assumed to have the same stress.

When one of the constituents is a liquid or gas with zero shear modulus, the Reuss average bulk and shear moduli for the composite are exactly the same as given by the Hashin–Shtrikman lower bound.

The Reuss average exactly describes the effective moduli of a suspension of solid grains in a fluid. It also describes the moduli of "shattered" materials in which solid fragments are completely surrounded by the pore fluid.

When all constituents are gases or liquids, or both, with zero shear modulus, the Reuss average gives the effective moduli of the mixture exactly.

In contrast to the Reuss average, which describes a number of real physical systems, real isotropic mixtures can never be as stiff as the Voigt bound (except for the single phase end members).

Mathematically the M in the Reuss average formula can represent any modulus: K, μ, E, and so forth. However, it makes most sense to compute only the

Reuss averages of the shear modulus, $M = \mu$, and the bulk modulus, $M = K$, and then compute the other moduli from these.

USES

The methods described in this section can be used for the following purposes:

- To compute the estimated range of average mineral modulus for a mixture of mineral grains.
- To compute the upper and lower bounds for a mixture of mineral and pore fluid.

ASSUMPTIONS AND LIMITATIONS

The methods described in this section presuppose that each constituent is isotropic, linear, elastic.

4.3 WOOD'S FORMULA

SYNOPSIS

In a fluid suspension or fluid mixture, where the heterogeneities are small compared with a wavelength, the sound velocity is given exactly by Wood's (1955) relation

$$V = \sqrt{\frac{K_R}{\rho}}$$

where K_R is the Reuss (isostress) average of the composite

$$\frac{1}{K_R} = \sum_{i=1}^{N} \frac{f_i}{K_i}$$

and ρ is the average density defined by

$$\rho = \sum_{i=1}^{N} f_i \rho_i$$

The f_i, K_i, and ρ_i are the volume fractions, bulk moduli, and densities of the phases, respectively.

EXAMPLE

Use Wood's relation to estimate the speed of sound in a water-saturated suspension of quartz particles at atmospheric conditions. The quartz properties are $K_{quartz} = 36$ GPa and $\rho_{quartz} = 2.65$ g/cm^3. The water properties are $K_{water} = 2.2$ GPa and $\rho_{water} = 1.0$ g/cm^3. The porosity is $\phi = 0.40$.

The Reuss average bulk modulus of the suspension is given by

$$K_{Reuss} = \left(\frac{\phi}{K_{water}} + \frac{1-\phi}{K_{quartz}}\right)^{-1} = \left(\frac{0.4}{2.2} + \frac{0.6}{36}\right)^{-1} = 5.04 \text{ GPa}$$

The density of the suspension is

$$\rho = \phi\rho_{water} + (1-\phi)\rho_{quartz} = (0.4)(1.0) + (0.6)(2.65) = 1.99 \text{ g/cm}^3$$

This gives the sound speed of

$$V = \sqrt{K/\rho} = \sqrt{5.04/1.99} = 1.59 \text{ km/s}$$

EXAMPLE

Use Wood's relation to estimate the speed of sound in a suspension of quartz particles in water with 50 percent saturation of air at atmospheric conditions. The quartz properties are $K_{quartz} = 36$ GPa and $\rho_{quartz} = 2.65$ g/cm^3. The water properties are $K_{water} = 2.2$ GPa and $\rho_{water} = 1.0$ g/cm^3. The air properties are $K_{air} = 0.000131$ GPa and $\rho_{air} = 0.00119$ g/cm^3. The porosity is $\phi = 0.40$.

The Reuss average bulk modulus of the suspension is given by

$$K_{Reuss} = \left(\frac{0.5\phi}{K_{water}} + \frac{0.5\phi}{K_{air}} + \frac{1-\phi}{K_{quartz}}\right)^{-1}$$

$$= \left(\frac{(0.5)(0.4)}{2.2} + \frac{(0.5)(0.4)}{0.000131} + \frac{0.6}{36}\right)^{-1} = 0.00065 \text{ GPa}$$

The density of the suspension is

$$\rho = 0.5\phi\rho_{water} + 0.5\phi\rho_{air} + (1-\phi)\rho_{quartz}$$

$$= (0.5)(0.4)(1.0) + (0.5)(0.4)(0.00119) + (0.6)(2.65) = 1.79 \text{ g/cm}^3$$

This gives the sound speed of

$$V = \sqrt{K/\rho} = \sqrt{0.00065/1.79} = 0.019 \text{ km/s}$$

USES

Wood's formula may be used to estimate the velocity in suspensions.

ASSUMPTIONS AND LIMITATIONS

Wood's formula presupposes that composite rock and each of its components are isotropic, linear, and elastic.

4.4 HILL AVERAGE MODULI ESTIMATE

SYNOPSIS

The Voigt–Reuss–Hill average is simply the arithmetic average of the Voigt upper bound and the Reuss lower bound. (See the discussion of the Voigt–Reuss bounds in Section 4.2.) This average is expressed as

$$M_{\mathrm{VRH}} = \frac{M_{\mathrm{V}} + M_{\mathrm{R}}}{2}$$

where

$$M_{\mathrm{V}} = \sum_{i=1}^{N} f_i M_i$$

$$\frac{1}{M_{\mathrm{R}}} = \sum_{i=1}^{N} \frac{f_i}{M_i}$$

The terms f_i and M_i are the volume fraction and modulus of the ith component, respectively. Although M can be any modulus, it makes most sense for it to be the shear modulus or the bulk modulus.

The Voigt–Reuss–Hill average is useful when an *estimate* of the moduli is needed, not just the allowable range of values. An obvious extension would be to average, instead, the Hashin–Shtrikman upper and lower bounds.

This resembles, but is not exactly the same as the average of the algebraic and harmonic means of velocity used by Greenberg and Castagna (1992) in their empirical V_{P}–V_{S} relation (see Section 7.8).

USES

The Voigt–Reuss–Hill average is used to estimate the effective elastic moduli of a rock in terms of its constituents and pore space.

ASSUMPTIONS AND LIMITATIONS

The following limitation and assumption apply to the Voigt–Reuss–Hill average:

- The result is strictly heuristic. Hill (1952) showed that the Voigt and Reuss averages are upper and low bounds, respectively. Several authors have shown that the average of these bounds can be a useful and sometimes accurate estimate of rock properties.
- The rock is isotropic.

4.5 COMPOSITE WITH UNIFORM SHEAR MODULUS

SYNOPSIS

Hill (1963) showed that when all of the phases or constituents in a composite have the same shear modulus, μ, the effective P-wave modulus, $M_{\mathrm{eff}} = (K_{\mathrm{eff}} + \frac{4}{3}\mu_{\mathrm{eff}})$, is given exactly by

$$\frac{1}{(K_{\mathrm{eff}} + \frac{4}{3}\mu_{\mathrm{eff}})} = \sum_{i=1}^{N} \frac{x_i}{(K_i + \frac{4}{3}\mu)} = \left\langle \frac{1}{K + \frac{4}{3}\mu} \right\rangle$$

where x_i is the volume fraction of the ith component, K_i is its bulk modulus, and $\langle\cdot\rangle$ refers to the volume average. Because $\mu_{\mathrm{eff}} = \mu_i = \mu$, any of the effective moduli can then be easily obtained.

This is obviously the same as

$$\frac{1}{(\rho V_{\mathrm{P}}^2)_{\mathrm{eff}}} = \left\langle \frac{1}{\rho V_{\mathrm{P}}^2} \right\rangle$$

This striking result states that the effective moduli of a composite with uniform shear modulus can be found *exactly* if one knows only the volume fractions of the constituents independent of the constituent geometries. There is no dependence, for example, on elllipsoids, spheres, or other idealized shapes.

Hill's equation follows simply from the expressions for Hashin–Shtrikman bounds (see Section 4.1 on Hashin–Shtrikman bounds) on the effective bulk modulus:

$$\frac{1}{K^{\mathrm{HS}\pm} + \frac{4}{3}\mu_{\{\substack{\max\\\min}\}}} = \left\langle \frac{1}{K + \frac{4}{3}\mu_{\{\substack{\max\\\min}\}}} \right\rangle$$

where $\mu_{\min}$ and $\mu_{\max}$ are the minimum and maximum shear moduli of the various constituents, yielding, respectively, the lower and upper bounds on the bulk modulus, $K^{\mathrm{HS}\pm}$. Any composite must have an effective bulk modulus that falls between the bounds. Because here $\mu = \mu_{\min} = \mu_{\max}$, the two bounds on the bulk modulus are equal and reduce to the Hill expression above.

In the case of a mixture of liquids or gases, or both, where $\mu = 0$ for all the constituents, the Hill's equation becomes the well-known isostress equation or Reuss average:

$$\frac{1}{K_{\mathrm{eff}}} = \sum_{i=1}^{N} \frac{x_i}{K_i} = \left\langle \frac{1}{K} \right\rangle$$

A somewhat surprising result is that a finely layered medium, where each layer is isotropic and has the same shear modulus but a different bulk modulus, is *isotropic* with a bulk modulus given by Hill's equation. (See Section 4.12 on the Backus average.)

USES

Hill's equation can be used to calculate the effective low-frequency moduli for rocks with spatially nonuniform or *patchy* saturation. At low frequencies, Gassmann's relations predict no change in the shear modulus between dry and saturated patches, allowing this relation to be used to estimate K.

ASSUMPTIONS AND LIMITATIONS

Hill's equation applies when the composite rock and each of its components are isotropic and have the same shear modulus.

4.6 ROCK AND PORE COMPRESSIBILITIES AND SOME PITFALLS

SYNOPSIS

This section summarizes useful relations among the compressibilities of porous materials and addresses some commonly made mistakes.

A nonporous elastic solid has a single compressibility

$$\beta = \frac{1}{V}\frac{\partial V}{\partial \sigma}$$

where σ is the hydrostatic stress applied on the outer surface and V is the sample bulk volume. In contrast, compressibilities for porous media are more complicated. We have to account for at least two pressures (the external confining pressure and the internal pore pressure) and two volumes (bulk volume and pore volume). Therefore, we can define at least four compressibilities. Following Zimmerman's (1991) notation, in which the first subscript indicates the volume change (b for bulk, p for pore) and the second subscript denotes the pressure that is varied (c for confining, p for pore), these compressibilities are

$$\beta_{\mathrm{bc}} = \frac{1}{V_{\mathrm{b}}}\left(\frac{\partial V_{\mathrm{b}}}{\partial \sigma_{\mathrm{c}}}\right)_{\sigma_{\mathrm{p}}}$$

$$\beta_{\mathrm{bp}} = -\frac{1}{V_{\mathrm{b}}}\left(\frac{\partial V_{\mathrm{b}}}{\partial \sigma_{\mathrm{p}}}\right)_{\sigma_{\mathrm{c}}}$$

$$\beta_{\mathrm{pc}} = \frac{1}{v_{\mathrm{p}}}\left(\frac{\partial v_{\mathrm{p}}}{\partial \sigma_{\mathrm{c}}}\right)_{\sigma_{\mathrm{p}}}$$

$$\beta_{\mathrm{pp}} = -\frac{1}{v_{\mathrm{p}}}\left(\frac{\partial v_{\mathrm{p}}}{\partial \sigma_{\mathrm{p}}}\right)_{\sigma_{\mathrm{c}}}$$

Note that the signs are chosen to ensure that the compressibilities are positive when tensional stress is taken to be positive. Thus, for instance, β_{bp} is to be interpreted as the fractional change in the bulk volume with respect to change in the pore pressure while the confining pressure is held constant. These are the *dry* or *drained* bulk and pore compressibilities. The effective dry bulk modulus is $K_{\mathrm{dry}} = 1/\beta_{\mathrm{bc}}$, and the dry-pore-space stiffness is $K_\phi = 1/\beta_{\mathrm{pc}}$. In addition, there is the *saturated* or *undrained* bulk compressibility when the mass of the pore fluid

is kept constant as the confining pressure changes:

$$\beta_u = \frac{1}{K_{sat\,low\,f}} = \frac{1}{V_b}\left(\frac{\partial V_b}{\partial \sigma_c}\right)_{m_{fluid}}$$

This equation assumes that the pore pressure is equilibrated throughout the pore space, and the expression is therefore appropriate for very low frequencies. At high frequencies, with unequilibrated pore pressures, the appropriate bulk modulus is $K_{sat\,hi\,f}$ calculated from some high-frequency theory such as the squirt, Biot, or inclusion models, or some other viscoelastic model.

The moduli K_{dry}, $K_{sat\,low\,f}$, $K_{sat\,hi\,f}$, and K_ϕ are the ones most useful in wave propagation rock physics. The other compressibilities are used in calculations of subsidence caused by fluid withdrawal and reservoir compressibility analyses. Some of the compressibilities can be related to each other by linear superposition and reciprocity. The well-known Gassmann's equation relates K_{dry} to K_{sat} through the mineral and fluid bulk moduli K_0 and K_f. A few other relations are (for simple derivations, see Zimmerman, 1991)

$$\beta_{bp} = \beta_{bc} - \frac{1}{K_0}$$

$$\beta_{pc} = \beta_{bp}/\phi$$

$$\beta_{pp} = \left[\beta_{bc} - (1+\phi)\frac{1}{K_0}\right]\Big/\phi$$

MORE ON DRY ROCK COMPRESSIBILITY

The effective dry rock compressibility of a homogeneous, linear, porous, elastic solid with any arbitrarily shaped pore space (sometimes called the "drained" or "frame" compressibility) can be written as

$$\frac{1}{K_{dry}} = \frac{1}{K_0} + \frac{1}{V_b}\frac{\partial v_p}{\partial \sigma_c}\bigg|_{\sigma_p}$$

or

$$\frac{1}{K_{dry}} = \frac{1}{K_0} + \frac{\phi}{K_\phi} \tag{1}$$

where

$$\frac{1}{K_\phi} = \frac{1}{v_p}\frac{\partial v_p}{\partial \sigma_c}\bigg|_{\sigma_p}$$

is defined as the dry pore space compressibility (K_ϕ is the dry pore space stiffness),

$K_{dry} = 1/\beta_{bc}$ = effective bulk modulus of dry porous solid
K_0 = bulk modulus of intrinsic mineral material
V_b = total bulk volume
v_p = pore volume
$\phi = v_p/V_b$ = porosity
σ_c, σ_p = hydrostatic confining stress and pore stress (pore pressure)

We assume that no inelastic effects such as friction or viscosity are present. These equations are strictly true, regardless of pore geometry and pore concentration.

CAUTION: "Dry rock" is not the same as gas-saturated rock. The dry-frame modulus refers to the incremental bulk deformation resulting from an increment of applied confining pressure while pore pressure is held constant. This corresponds to a "drained" experiment in which pore fluids can flow freely in or out of the sample to ensure constant pore pressure. Alternatively, it can correspond to an undrained experiment in which the pore fluid has zero bulk modulus and thus the pore compressions do not induce changes in pore pressure, which is approximately the case for an air-filled sample at standard temperature and pressure. However, at reservoir conditions (high pore pressure), gas takes on a nonnegligible bulk modulus and should be treated as a saturating fluid.

CAUTION: The harmonic average of the mineral and dry pore moduli, which resembles equation (1) above, is incorrect:

$$\frac{1}{K_{dry}} \stackrel{?}{=} \frac{1-\phi}{K_0} + \frac{\phi}{K_\phi} \quad \textbf{(incorrect)}$$

This equation is sometimes "guessed" because it resembles the Reuss average, but it has no justification from elasticity analysis. It is also *incorrect* to write

$$\frac{1}{K_{dry}} \stackrel{?}{=} \frac{1}{K_0} + \frac{\partial \phi}{\partial \sigma_c} \quad \textbf{(incorrect)} \tag{2}$$

The correct expression is

$$\frac{1}{K_{dry}} = \frac{1}{(1-\phi)}\left(\frac{1}{K_0} + \frac{\partial \phi}{\partial \sigma_c}\right)$$

The incorrect equation (2) appears as an intermediate result in some of the classic literature of rock physics. The notable final results are still correct, for the actual derivations are done in terms of the pore volume change, $\partial v_p/\partial \sigma_c$, and not $\partial \phi/\partial \sigma_c$.

Not distinguishing between changes in differential (effective) pressure, $\sigma_d = \sigma_c - \sigma_p$, and confining pressure, σ_c, can lead to confusion. Changing σ_c while σ_p

is kept constant ($\delta\sigma_p = 0$) is not the same as changing σ_c with $\delta\sigma_p = \delta\sigma_c$ (i.e., the differential stress is kept constant). In the first situation the porous medium deforms with the effective dry modulus K_{dry}. The second situation is one of uniform hydrostatic pressure outside *and* inside the porous rock. For this stress state the rock deforms with the intrinsic mineral modulus K_0. Not understanding this can lead to the following erroneous results:

$$\frac{1}{K_0} \stackrel{?}{=} \frac{1}{K_{dry}} - \frac{1}{(1-\phi)}\frac{\partial\phi}{\partial\sigma_c} \quad \textbf{(incorrect)}$$

or

$$\frac{\partial\phi}{\partial\sigma_c} \stackrel{?}{=} (1-\phi)\left(\frac{1}{K_{dry}} - \frac{1}{K_0}\right) \quad \textbf{(incorrect)}$$

TABLE 4.6.1. Correct and incorrect versions of the fundamental equations.

Incorrect	Correct
$\frac{1}{K_{dry}} \stackrel{?}{=} \frac{1}{K_0} + \frac{\partial\phi}{\partial\sigma_c}$	$\frac{1}{K_{dry}} = \frac{1}{K_0} + \frac{1}{V_b}\frac{\partial v_p}{\partial\sigma_c}$
$\frac{1}{K_{dry}} \stackrel{?}{=} \frac{1-\phi}{K_0} + \frac{\phi}{K_\phi}$	$\frac{1}{K_{dry}} = \frac{1}{K_0} + \frac{\phi}{K_\phi}$
$\frac{1}{K_{dry}} \stackrel{?}{=} \frac{1}{K_0} + \frac{1}{(1-\phi)}\frac{\partial\phi}{\partial\sigma_c}$	$\frac{1}{K_{dry}} = \frac{1}{(1-\phi)}\left(\frac{1}{K_0} + \frac{\partial\phi}{\partial\sigma_c}\right)$
$\frac{\partial\phi}{\partial\sigma_c} \stackrel{?}{=} \left(\frac{1}{K_{dry}} - \frac{1}{K_0}\right)(1-\phi)$	$\frac{\partial\phi}{\partial\sigma_c} = \frac{1-\phi}{K_{dry}} - \frac{1}{K_0}$

ASSUMPTIONS AND LIMITATIONS

The following presuppositions apply to the equations presented in this section:

- They assume isotropic, linear, porous, elastic media.
- All derivations here are in the context of linear elasticity with infinitesimal, incremental strains and stresses. Hence Eulerian and Lagrangian formulations are equivalent.
- It is assumed that the temperature is always held constant as the pressure varies.
- Inelastic effects such as friction and viscosity are neglected.

4.7 KUSTER AND TOKSÖZ FORMULATION FOR EFFECTIVE MODULI

SYNOPSIS

Kuster and Toksöz (1974) derived expressions for P- and S- wave velocities by using a long-wavelength first-order scattering theory. A generalization of their expressions for the effective moduli K^*_{KT} and μ^*_{KT} for a variety of inclusion shapes can be written as (Kuster and Toksöz, 1974; Berryman, 1980b)

$$(K^*_{KT} - K_m)\frac{(K_m + \frac{4}{3}\mu_m)}{(K^*_{KT} + \frac{4}{3}\mu_m)} = \sum_{i=1}^{N} x_i(K_i - K_m)P^{mi}$$

$$(\mu^*_{KT} - \mu_m)\frac{(\mu_m + \zeta_m)}{(\mu^*_{KT} + \zeta_m)} = \sum_{i=1}^{N} x_i(\mu_i - \mu_m)Q^{mi}$$

where the summation is over the different inclusion types with volume concentration x_i, and

$$\zeta = \frac{\mu(9K + 8\mu)}{6(K + 2\mu)}$$

The coefficients P^{mi} and Q^{mi} describe the effect of an inclusion of material i in a background medium m. For example, a two-phase material with a single type of inclusion embedded within a background medium has a single term on the right-hand side. Inclusions with different material properties or different shapes require separate terms in the summation. Each set of inclusions must be distributed randomly, and thus its effect is isotropic. These formulas are uncoupled and can be made explicit for easy evaluation. Table 4.7.1 gives expressions for P and Q for some simple inclusion shapes.

Dry cavities can be modeled by setting the inclusion moduli to zero. Fluid-saturated cavities are simulated by setting the inclusion shear modulus to zero.

CAUTION: Because the cavities are isolated with respect to flow, this approach simulates very high frequency saturated rock behavior appropriate to ultrasonic laboratory conditions. At low frequencies, when there is time for wave-induced pore pressure increments to flow and equilibrate, it is better to find the effective moduli for dry cavities and then saturate them with the Gassmann low-frequency relations (see Section 6.3). This should not be confused with the tendency to term this approach a low-frequency theory, for crack dimensions are assumed to be much smaller than a wavelength.

EXAMPLE

Calculate the effective bulk and shear moduli, K^*_{KT} and μ^*_{KT}, for a quartz matrix with spherical, water-filled inclusions of porosity 0.1.

$K_m = 37$ GPa, $\mu_m = 44$ GPa, $K_i = 2.25$ GPa, $\mu_i = 0$ GPa.

Volume fraction of spherical inclusions $x_1 = 0.1$ and $N = 1$. The P and Q values for spheres are obtained from the table as follows:

$$P^{mi} = \frac{\left(37 + \frac{4}{3}44\right)}{\left(2.25 + \frac{4}{3}44\right)} = 1.57$$

$$\zeta_m = \frac{44(9 \times 37 + 8 \times 44)}{6(37 + 2 \times 44)} = 40.2$$

$$Q^{mi} = \frac{(44 + 40.2)}{(0 + 40.2)} = 2.095$$

Substituting these in the Kuster–Toksöz equations gives:

$$K^*_{KT} = 31.84 \text{ GPa}, \quad \mu^*_{KT} = 35.7 \text{ GPa}$$

TABLE 4.7.1. Coefficients P and Q for some specific shapes. The subscripts m and i refer to the background and inclusion materials [from Berryman (1995)].

Inclusion Shape	P^{mi}	Q^{mi}
Spheres	$\dfrac{K_m + \frac{4}{3}\mu_m}{K_i + \frac{4}{3}\mu_m}$	$\dfrac{\mu_m + \zeta_m}{\mu_i + \zeta_m}$
Needles	$\dfrac{K_m + \mu_m + \frac{1}{3}\mu_i}{K_i + \mu_m + \frac{1}{3}\mu_i}$	$\dfrac{1}{5}\left(\dfrac{4\mu_m}{\mu_m + \mu_i} + 2\dfrac{\mu_m + \gamma_m}{\mu_i + \gamma_m} + \dfrac{K_i + \frac{4}{3}\mu_m}{K_i + \mu_m + \frac{1}{3}\mu_i}\right)$
Disks	$\dfrac{K_m + \frac{4}{3}\mu_i}{K_i + \frac{4}{3}\mu_i}$	$\dfrac{\mu_m + \zeta_i}{\mu_i + \zeta_i}$
Penny cracks	$\dfrac{K_m + \frac{4}{3}\mu_i}{K_i + \frac{4}{3}\mu_i + \pi\alpha\beta_m}$	$\dfrac{1}{5}\left(1 + \dfrac{8\mu_m}{4\mu_i + \pi\alpha(\mu_m + 2\beta_m)} + 2\dfrac{K_i + \frac{2}{3}(\mu_i + \mu_m)}{K_i + \frac{4}{3}\mu_i + \pi\alpha\beta_m}\right)$

$$\beta = \mu\frac{(3K + \mu)}{(3K + 4\mu)} \quad \gamma = \mu\frac{(3K + \mu)}{(3K + 7\mu)} \quad \zeta = \frac{\mu}{6}\frac{(9K + 8\mu)}{(K + 2\mu)}$$

The P and Q values for ellipsoidal inclusions with arbitrary aspect ratio are the same as given in Section 4.8 on self-consistent methods.

Note that for spherical inclusions, the Kuster–Toksöz expressions for bulk modulus are identical to the Hashin–Shtrikman upper bound even though the Kuster–Toksöz expressions are formally limited to low porosity.

ASSUMPTIONS AND LIMITATIONS

The following presuppositions and limitations apply to the Kuster–Toksöz formulations:

- They assume isotropic, linear, elastic media.
- They are limited to dilute concentrations of the inclusions.
- They assume idealized ellipsoidal inclusion shapes.

4.8 SELF-CONSISTENT APPROXIMATIONS OF EFFECTIVE MODULI

SYNOPSIS

Theoretical estimates of the effective moduli of composite or porous elastic materials generally depend on (1) the properties of the individual components of the composite, (2) the volume fractions of the components, and (3) the geometric details of the shapes and spatial distributions of the components. The bounding methods (see discussions of the Hashin–Shtrikman and Voigt–Reuss bounds, Sections 4.1 and 4.2) establish upper and lower bounds when only (1) and (2) are known with no geometric details. A second approach improves these estimates by adding statistical information about the phases (e.g., Beran and Molyneux, 1966; McCoy, 1970; Corson, 1974; Watt, Davies, and O'Connell, 1976). A third approach is to assume very specific inclusion shapes. Most methods use the solution for the elastic deformation of a single inclusion of one material in an infinite background medium of the second material and then use one scheme or another to estimate the effective moduli when there is a distribution of these inclusions. These estimates are generally limited to dilute distributions of inclusions owing to the difficulty of modeling or estimating the elastic interaction of inclusions in close proximity.

A relatively successful, and certainly popular, method to extend these specific geometry methods to slightly higher concentrations of inclusions is the

self-consistent approximation (Budiansky, 1965; Hill, 1965; Wu, 1966). In this approach one still uses the mathematical solution for the deformation of isolated inclusions, but the interaction of inclusions is approximated by replacing the background medium with the as-yet-unknown effective medium. These methods were made popular following a series of papers by O'Connell and Budiansky (see, for example, O'Connell and Budiansky, 1974). Their equations for effective bulk and shear moduli, K^*_{SC} and μ^*_{SC}, respectively, of a cracked medium with randomly oriented dry penny-shaped cracks (in the limiting case when the aspect ratio α goes to 0) are

$$\frac{K^*_{SC}}{K} = 1 - \frac{16}{9}\left(\frac{1-\nu^{*2}_{SC}}{1-2\nu^*_{SC}}\right)\varepsilon$$

$$\frac{\mu^*_{SC}}{\mu} = 1 - \frac{32}{45}\frac{(1-\nu^*_{SC})(5-\nu^*_{SC})}{(2-\nu^*_{SC})}\varepsilon$$

where K and μ are the bulk and shear moduli, respectively, of the uncracked medium, and ε is the crack density parameter, which is defined as the number of cracks per unit volume times the crack radius cubed. The effective Poisson ratio ν^*_{SC} is related to ε and the Poisson's ratio ν of the uncracked solid by

$$\varepsilon = \frac{45}{16}\frac{(\nu-\nu^*_{SC})(2-\nu^*_{SC})}{(1-\nu^{*2}_{SC})(10\nu - 3\nu\nu^*_{SC} - \nu^*_{SC})}$$

This equation must first be solved for ν^*_{SC} for a given ε, after which K^*_{SC} and μ^*_{SC} can be evaluated. The nearly linear dependence of ν^*_{SC} on ε is well approximated by

$$\nu^*_{SC} = \nu\left(1 - \frac{16}{9}\varepsilon\right)$$

and this simplifies the calculation of the effective moduli. For fluid-saturated, infinitely thin penny-shaped cracks

$$\frac{K^*_{SC}}{K} = 1$$

$$\frac{\mu^*_{SC}}{\mu} = 1 - \frac{32}{15}\left(\frac{1-\nu^*_{SC}}{2-\nu^*_{SC}}\right)\varepsilon$$

$$\varepsilon = \frac{45}{32}\frac{(\nu^*_{SC}-\nu)(2-\nu^*_{SC})}{(1-\nu^{*2}_{SC})(1-2\nu)}$$

However, this result is inadequate for small aspect ratio cracks with soft-fluid saturation, such as when the parameter $\omega = K_{fluid}/(\alpha K)$ is of the order 1. Then the appropriate equations given by O'Connell and Budiansky are

$$\frac{K^*_{SC}}{K} = 1 - \frac{16}{9}\frac{(1-\nu^{*2}_{SC})}{(1-2\nu^*_{SC})}D\varepsilon$$

$$\frac{\mu^*_{SC}}{\mu} = 1 - \frac{32}{45}(1-\nu^*_{SC})\left[D + \frac{3}{(2-\nu^*_{SC})}\right]\varepsilon$$

$$\varepsilon = \frac{45}{16}\frac{(\nu-\nu^*_{SC})}{(1-\nu^{*2}_{SC})}\frac{(2-\nu^*_{SC})}{[D(1+3\nu)(2-\nu^*_{SC}) - 2(1-2\nu)]}$$

$$D = \left[1 + \frac{4}{3\pi}\frac{(1-\nu^{*2}_{SC})}{(1-2\nu^*_{SC})}\frac{K}{K^*_{SC}}\omega\right]^{-1}$$

Wu's self-consistent modulus estimates for two-phase composites may be expressed as (m = matrix, i = inclusion)

$$K^*_{SC} = K_m + x_i(K_i - K_m)P^{*i}$$

$$\mu^*_{SC} = \mu_m + x_i(\mu_i - \mu_m)Q^{*i}$$

Berryman (1980b, 1995) gives a more general form of the self-consistent approximations for N-phase composites:

$$\sum_{i=1}^{N} x_i(K_i - K^*_{SC})P^{*i} = 0$$

$$\sum_{i=1}^{N} x_i(\mu_i - \mu^*_{SC})Q^{*i} = 0$$

where i refers to the ith material, x_i is its volume fraction, P and Q are geometric factors given in Table 4.8.1, and the superscript $*i$ on P and Q indicates that the factors are for an inclusion of material i in a background medium with self-consistent effective moduli K^*_{SC} and μ^*_{SC}. These equations are coupled and must be solved by simultaneous iteration. Although Berryman's self-consistent method does not converge for fluid disks ($\mu_2 = 0$), the formulas for penny-shaped fluid-filled cracks are generally not singular and converge rapidly. However, his estimates for needles, disks, and penny cracks should be used cautiously for fluid-saturated composite materials.

Dry cavities can be modeled by setting the inclusion moduli to zero. Fluid-saturated cavities are simulated by setting the inclusion shear modulus to zero.

CAUTION: Because the cavities are isolated with respect to flow, this approach simulates very-high-frequency saturated rock behavior appropriate to ultrasonic laboratory conditions. At low frequencies, when there is time for wave-induced pore pressure increments to flow and equilibrate, it is better to find the effective moduli for dry cavities and then saturate them with the Gassmann low-frequency relations. This should not be confused with the tendency to term this approach a low-frequency theory, for crack dimensions are assumed to be much smaller than a wavelength.

TABLE 4.8.1. Coefficients P and Q for some specific shapes. The subscripts m and i refer to the background and inclusion materials [from Berryman (1995)].

Inclusion Shape	P^{mi}	Q^{mi}
Spheres	$\dfrac{K_m+\frac{4}{3}\mu_m}{K_i+\frac{4}{3}\mu_m}$	$\dfrac{\mu_m+\zeta_m}{\mu_i+\zeta_m}$
Needles	$\dfrac{K_m+\mu_m+\frac{1}{3}\mu_i}{K_i+\mu_m+\frac{1}{3}\mu_i}$	$\dfrac{1}{5}\left(\dfrac{4\mu_m}{\mu_m+\mu_i}+2\dfrac{\mu_m+\gamma_m}{\mu_i+\gamma_m}+\dfrac{K_i+\frac{4}{3}\mu_m}{K_i+\mu_m+\frac{1}{3}\mu_i}\right)$
Disks	$\dfrac{K_m+\frac{4}{3}\mu_i}{K_i+\frac{4}{3}\mu_i}$	$\dfrac{\mu_m+\zeta_i}{\mu_i+\zeta_i}$
Penny cracks	$\dfrac{K_m+\frac{4}{3}\mu_i}{K_i+\frac{4}{3}\mu_i+\pi\alpha\beta_m}$	$\dfrac{1}{5}\left[1+\dfrac{8\mu_m}{4\mu_i+\pi\alpha(\mu_m+2\beta_m)}+2\dfrac{K_i+\frac{2}{3}(\mu_i+\mu_m)}{K_i+\frac{4}{3}\mu_i+\pi\alpha\beta_m}\right]$

$$\beta=\mu\frac{(3K+\mu)}{(3K+4\mu)}\quad \gamma=\mu\frac{(3K+\mu)}{(3K+7\mu)}\quad \zeta=\frac{\mu}{6}\frac{(9K+8\mu)}{(K+2\mu)}$$

EXAMPLE

Calculate the self-consistent effective bulk and shear moduli, K^*_{SC} and μ^*_{SC}, for a water-saturated rock consisting of spherical quartz grains (aspect ratio $\alpha_1=1$) and total porosity 0.3. The pore space consists of spherical pores ($\alpha_2=1$) and thin penny-shaped cracks ($\alpha_3=10^{-2}$). The thin cracks have a porosity of 0.01, whereas the remaining porosity (0.29) is made up of the spherical pores.

The total number of phases, N, is 3.

K_1(quartz) = 37 GPa, μ_1(quartz) = 44 GPa,
$\alpha_1=1$, x_1 (volume fraction) = 0.7
K_2(water, spherical pores) = 2.25 GPa,
μ_2(water, spherical pores) = 0 GPa,
α_2(spherical pores) = 1, x_2 (volume fraction) = 0.29
K_3(water, thin cracks) = 2.25 GPa,
μ_3(water, thin cracks) = 0 GPa,
α_3(thin cracks) = 10^{-2}, x_3 (volume fraction) = 0.01

The coupled equations for K^*_{SC} and μ^*_{SC} are

$$x_1(K_1-K^*_{SC})P^{*1}+x_2(K_2-K^*_{SC})P^{*2}+x_3(K_3-K^*_{SC})P^{*3}=0$$

$$x_1(\mu_1-\mu^*_{SC})Q^{*1}+x_2(\mu_2-\mu^*_{SC})Q^{*2}+x_3(\mu_3-\mu^*_{SC})Q^{*3}=0$$

The P's and Q's are obtained from Table 4.8.1 or from the more general equation for ellipsoids of arbitrary aspect ratio. In the equations for P's and Q's, K_m and μ_m are replaced everywhere by K^*_{SC} and μ^*_{SC}, respectively. The coupled equations are solved iteratively, starting from some initial guess for K^*_{SC} and μ^*_{SC}. The Voigt average may be taken as the starting point. The converged solutions (known as the fixed points of the coupled equations) are $K^*_{SC}=16.8$ GPa and $\mu^*_{SC}=11.6$ GPa.

The coefficients P and Q for ellipsoidal inclusions of arbitrary aspect ratio are given by

$$P=\frac{1}{3}T_{iijj}$$

$$Q=\frac{1}{5}\left(T_{ijij}-\frac{1}{3}T_{iijj}\right)$$

where the tensor T_{ijkl} relates the uniform far-field strain field to the strain within the ellipsoidal inclusion (Wu, 1966). Berryman (1980b) gives the pertinent scalars required for computing P and Q as

$$T_{iijj}=3F_1/F_2$$

$$T_{ijij}-\frac{1}{3}T_{iijj}=\frac{2}{F_3}+\frac{1}{F_4}+\frac{F_4F_5+F_6F_7-F_8F_9}{F_2F_4}$$

where

$$F_1=1+A\left[\frac{3}{2}(f+\theta)-R\left(\frac{3}{2}f+\frac{5}{2}\theta-\frac{4}{3}\right)\right]$$

$$F_2=1+A\left[1+\frac{3}{2}(f+\theta)-(R/2)(3f+5\theta)\right]+B(3-4R)$$
$$+(A/2)(A+3B)(3-4R)[f+\theta-R(f-\theta+2\theta^2)]$$

$$F_3=1+A\left[1-\left(f+\frac{3}{2}\theta\right)+R(f+\theta)\right]$$

$$F_4=1+(A/4)[f+3\theta-R(f-\theta)]$$

$$F_5=A\left[-f+R\left(f+\theta-\frac{4}{3}\right)\right]+B\theta(3-4R)$$

$$F_6=1+A[1+f-R(f+\theta)]+B(1-\theta)(3-4R)$$

$$F_7=2+(A/4)[3f+9\theta-R(3f+5\theta)]+B\theta(3-4R)$$

$$F_8 = A[1 - 2R + (f/2)(R - 1) + (\theta/2)(5R - 3)] + B(1 - \theta)(3 - 4R)$$
$$F_9 = A[(R - 1)f - R\theta] + B\theta(3 - 4R)$$

with A, B, and R given by

$$A = \mu_i/\mu_m - 1$$
$$B = \frac{1}{3}(K_i/K_m - \mu_i/\mu_m)$$

and

$$R = [(1 - 2\nu_m)/2(1 - \nu_m)]$$

The functions θ and f are given by

$$\theta = \begin{cases} \frac{\alpha}{(\alpha^2-1)^{3/2}}[\alpha(\alpha^2 - 1)^{1/2} - \cosh^{-1}\alpha] \\ \frac{\alpha}{(1-\alpha^2)^{3/2}}[\cos^{-1}\alpha - \alpha(1 - \alpha^2)^{1/2}] \end{cases}$$

for prolate and oblate spheroids, respectively, and

$$f = \frac{\alpha^2}{1 - \alpha^2}(3\theta - 2)$$

Note that $\alpha < 1$ for oblate spheroids, and $\alpha > 1$ for prolate spheroids.

ASSUMPTIONS AND LIMITATIONS

The approach described in this section has the following presuppositions:

- Idealized ellipsoidal inclusion shapes.
- Isotropic, linear, elastic media.
- Cracks are isolated with respect to fluid flow. Pore pressures are unequilibrated and adiabatic. Appropriate for high-frequency laboratory conditions. For low-frequency field situations use dry inclusions and then saturate by using Gassmann relations. This should not be confused with the tendency to term this approach a low-frequency theory, for crack dimensions are assumed to be much smaller than a wavelength.

4.9 DIFFERENTIAL EFFECTIVE MEDIUM MODEL

SYNOPSIS

The differential effective medium (DEM) theory models two-phase composites by incrementally adding inclusions of one phase (phase 2) to the matrix phase (Cleary et al., 1980; Norris, 1985; Zimmerman, 1991). The matrix begins as phase 1 (when concentration of phase 2 is zero) and is changed at each step as a new increment of phase 2 material is added. The process is continued until the desired proportion of the constituents is reached. The DEM formulation does not treat each constituent symmetrically. There is a preferred matrix or host material, and the effective moduli depend on the construction path taken to reach the final composite. Starting with material 1 as the host and incrementally adding inclusions of material 2 will not, in general, lead to the same effective properties as starting with phase 2 as the host. For multiple inclusion shapes or multiple constituents, the effective moduli depend not only on the final volume fractions of the constituents but also on the order in which the incremental additions are done. The process of incrementally adding inclusions to the matrix is really a thought experiment and should not be taken to provide an accurate description of the true evolution of rock porosity in nature.

The coupled system of ordinary differential equations for the effective bulk and shear moduli, K^* and μ^*, respectively, are (Berryman, 1992)

$$(1 - y)\frac{d}{dy}[K^*(y)] = (K_2 - K^*)P^{(*2)}(y)$$
$$(1 - y)\frac{d}{dy}[\mu^*(y)] = (\mu_2 - \mu^*)Q^{(*2)}(y)$$

with initial conditions $K^*(0) = K_1$ and $\mu^*(0) = \mu_1$, where

K_1, μ_1 = bulk and shear moduli of the initial host material (phase 1)
K_2, μ_2 = bulk and shear moduli of the incrementally added inclusions (phase 2)
y = concentration of phase 2

For fluid inclusions and voids, y equals the porosity, ϕ. The terms P and Q are geometric factors given in Table 4.9.1, and the superscript ^{*2} on P and

TABLE 4.9.1. Coefficients P and Q for some specific shapes. The subscripts m and i refer to the background and inclusion materials [from Berryman (1995)].

Inclusion Shape	P^{mi}	Q^{mi}
Spheres	$\dfrac{K_m + \frac{4}{3}\mu_m}{K_i + \frac{4}{3}\mu_m}$	$\dfrac{\mu_m + \zeta_m}{\mu_i + \zeta_m}$
Needles	$\dfrac{K_m + \mu_m + \frac{1}{3}\mu_i}{K_i + \mu_m + \frac{1}{3}\mu_i}$	$\dfrac{1}{5}\left(\dfrac{4\mu_m}{\mu_m + \mu_i} + 2\dfrac{\mu_m + \gamma_m}{\mu_i + \gamma_m} + \dfrac{K_i + \frac{4}{3}\mu_m}{K_i + \mu_m + \frac{1}{3}\mu_i}\right)$
Disks	$\dfrac{K_m + \frac{4}{3}\mu_i}{K_i + \frac{4}{3}\mu_i}$	$\dfrac{\mu_m + \zeta_i}{\mu_i + \zeta_i}$
Penny cracks	$\dfrac{K_m + \frac{4}{3}\mu_i}{K_i + \frac{4}{3}\mu_i + \pi\alpha\beta_m}$	$\dfrac{1}{5}\left[1 + \dfrac{8\mu_m}{4\mu_i + \pi\alpha(\mu_m + 2\beta_m)} + 2\dfrac{K_i + \frac{2}{3}(\mu_i + \mu_m)}{K_i + \frac{4}{3}\mu_i + \pi\alpha\beta_m}\right]$

$$\beta = \mu\frac{(3K+\mu)}{(3K+4\mu)} \quad \gamma = \mu\frac{(3K+\mu)}{(3K+7\mu)} \quad \zeta = \frac{\mu}{6}\frac{(9K+8\mu)}{(K+2\mu)}$$

Q indicates that the factors are for an inclusion of material 2 in a background medium with effective moduli K^* and μ^*. Dry cavities can be modeled by setting the inclusion moduli to zero. Fluid-saturated cavities are simulated by setting the inclusion shear modulus to zero.

CAUTION: Because the cavities are isolated with respect to flow, this approach simulates very-high-frequency saturated rock behavior appropriate to ultrasonic laboratory conditions. At low frequencies, when there is time for wave-induced pore pressure increments to flow and equilibrate, it is better to find the effective moduli for dry cavities and then saturate them with the Gassmann low-frequency relations. This should not be confused with the tendency to term this approach a low-frequency theory, for inclusion dimensions are assumed to be much smaller than a wavelength.

The P and Q for ellipsoidal inclusions with arbitrary aspect ratio are the same as given in Section 4.8 for the self-consistent methods.

Norris et al. (1985) have shown that the DEM is realizable and therefore is always consistent with the Hashin–Shtrikman upper and lower bounds.

The derivation of the DEM equations as given above (Norris, 1985; Berryman, 1992) assumes that, as each new inclusion (or pore) is introduced, it displaces on average either the host matrix material or the inclusion material with probabilities $(1 - y)$ and y, respectively. A slightly different derivation by Zimmerman (1984) assumed that when a new inclusion is introduced, it always displaces the host material alone. This leads to similar differential equations with $dy/(1 - y)$ replaced by dy. The effective moduli predicted by the Zimmerman version of DEM

are always slightly stiffer (for the same inclusion geometry and concentration) than the DEM equations given above. They both predict the same first-order terms in y but begin to diverge at concentrations above 10 percent. The dependence of effective moduli on concentration goes as $e^{-2y} = (1 - 2y + 2y^2 - ...)$ for Zimmerman's equations, whereas it behaves as $(1 - y)^2 = (1 - 2y + 2y^2 - ...)$ for the Norris version. In general, for a fixed inclusion geometry and porosity, the Zimmerman DEM effective moduli are close to the Kuster–Toksöz effective moduli and are stiffer than the Norris–Berryman DEM predictions, which in turn are stiffer than the Berryman self-consistent effective moduli. For spherical inclusions, the Zimmerman estimates fall above the Hashin–Shtrikman upper bound for high concentrations.

An important conceptual difference between the DEM and self-consistent schemes for calculating effective moduli of composites is that the DEM scheme identifies one of the constituents as a host or matrix material in which inclusions of the other constituent(s) are embedded, whereas the self-consistent scheme does not identify any specific host material but treats the composite as an aggregate of all the constituents.

MODIFIED DEM WITH CRITICAL POROSITY CONSTRAINTS

In the usual DEM model, starting from a solid initial host, a porous material stays intact at all porosities and falls apart only at the very end when $y = 1$ (100-percent porosity). This is because the solid host remains connected and therefore load bearing.

Although DEM is a good model for materials such as glass foam (Berge, Berryman, and Bonner, 1993) and oceanic basalts (Berge, Fryer, and Wilkens, 1992), most reservoir rocks fall apart at a critical porosity, ϕ_c, significantly less than 1.0 and are not represented very well by the conventional DEM theory. The modified DEM model (Mukerji et al., 1995) incorporates percolation behavior at any desired ϕ_c by redefining the phase 2 end member. The inclusions are now no longer made up of pure fluid (the original phase 2 material) but are composite inclusions of the critical phase at ϕ_c with elastic moduli (K_c, μ_c). With this definition, y denotes the concentration of the critical phase in the matrix. The total porosity is given by $\phi = y\phi_c$.

The computations are implemented by replacing (K_2, μ_2) with (K_c, μ_c) everywhere in the equations. Integrating along the reverse path, from $\phi = \phi_c$ to $\phi = 0$ gives lower moduli, for now the softer critical phase is the matrix. The moduli of the critical phase may be taken as the Reuss average value at ϕ_c of the pure end member moduli. Because the critical phase consists of grains just barely touching each other, better estimates of K_c and μ_c may be obtained from measurements

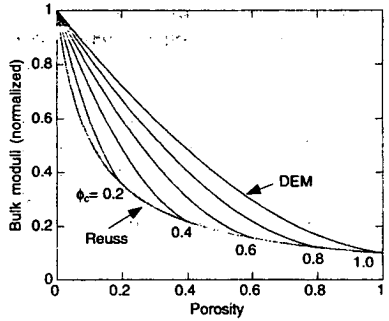

Figure 4.9.1

on loose sands or from models of granular material. For porosities greater than ϕ_c, the material is a suspension and is best characterized by the Reuss average (or Wood's equation).

Figure 4.9.1 shows normalized bulk moduli curves for the conventional DEM theory (percolation at $\phi = 1$) and for the modified DEM (percolation at $\phi_c < 1$) for a range of ϕ_c values. When $\phi_c = 1$, the modified DEM coincides with the conventional DEM curve. The shapes of the inclusions were taken to be spheres. The path was from 0 to ϕ_c and (K_c, μ_c) were taken as the Reuss average values at ϕ_c. For this choice of (K_c, μ_c), estimates along the reversed path coincide with the Reuss curve.

USES

The purpose of the differential effective medium model is to estimate the effective elastic moduli of a rock in terms of its constituents and pore space.

ASSUMPTIONS AND LIMITATIONS

The following assumptions and limitations apply to the differential effective medium model:

- The rock is isotropic, linear, elastic.
- The process of incrementally adding inclusions to the matrix is a thought experiment and should not be taken to provide an accurate description of the true evolution of rock porosity in nature.

- Idealized ellipsoidal inclusion shapes are assumed.
- Cracks are isolated with respect to fluid flow. Pore pressures are unequilibrated and adiabatic. The model is appropriate for high-frequency laboratory conditions. For low-frequency field situations, use dry inclusions and then saturate by using Gassmann relations. This should not be confused with the tendency to term this approach a low-frequency theory, for crack dimensions are assumed to be much smaller than a wavelength.

4.10 HUDSON'S MODEL FOR CRACKED MEDIA

SYNOPSIS

Hudson's model is based on a scattering theory analysis of the mean wave field in an elastic solid with thin, penny-shaped ellipsoidal cracks or inclusions (Hudson, 1980, 1981). The effective moduli c_{ij}^{eff} are given as

$$c_{ij}^{\text{eff}} = c_{ij}^0 + c_{ij}^1 + c_{ij}^2$$

where c_{ij}^0 are the isotropic background moduli, and c_{ij}^1, c_{ij}^2 are the first- and second-order corrections, respectively. (See Section 2.2 on anisotropy for the two-index notation of elastic moduli. Note also that Hudson uses a slightly different definition and that there is an extra factor of 2 in his c_{44}, c_{55}, and c_{66}. This makes the equations given in his paper for c_{44}^1 and c_{44}^2 slightly different from those given below, which are consistent with the more standard notation described in Section 2.2 on anisotropy.)

For a single crack set with crack normals aligned along the 3-axis, the cracked media show transverse isotropic symmetry, and the corrections are

$$c_{11}^1 = -\frac{\lambda^2}{\mu}\varepsilon U_3$$

$$c_{13}^1 = -\frac{\lambda(\lambda + 2\mu)}{\mu}\varepsilon U_3$$

$$c_{33}^1 = -\frac{(\lambda + 2\mu)^2}{\mu}\varepsilon U_3$$

$$c_{44}^1 = -\mu\varepsilon U_1$$

$$c_{66}^1 = 0$$

and (superscripts on the c_{ij} denote second order, not quantities squared)

$$c_{11}^2 = \frac{q}{15}\frac{\lambda^2}{(\lambda+2\mu)}(\varepsilon U_3)^2$$

$$c_{13}^2 = \frac{q}{15}\lambda(\varepsilon U_3)^2$$

$$c_{33}^2 = \frac{q}{15}(\lambda+2\mu)(\varepsilon U_3)^2$$

$$c_{44}^2 = \frac{2}{15}\frac{\mu(3\lambda+8\mu)}{\lambda+2\mu}(\varepsilon U_1)^2$$

$$c_{66}^2 = 0$$

where

$$q = 15\frac{\lambda^2}{\mu^2} + 28\frac{\lambda}{\mu} + 28$$

$$\varepsilon = \frac{N}{V}a^3 = \frac{3\phi}{4\pi\alpha} = \text{crack density}$$

The isotropic background elastic moduli are λ and μ, and a and α are the crack radius and aspect ratio, respectively. The corrections c_{ij}^1 and c_{ij}^2 obey the usual symmetry properties for transverse isotropy or hexagonal symmetry (see Section 2.2 on anisotropy). The terms U_1 and U_3 depend on the crack conditions. For dry cracks

$$U_1 = \frac{16(\lambda+2\mu)}{3(3\lambda+4\mu)}$$

$$U_3 = \frac{4(\lambda+2\mu)}{3(\lambda+\mu)}$$

For "weak" inclusions (i.e., when $\mu\alpha/[K'+(4/3)\mu']$ is of the order 1 and is not small enough to be neglected)

$$U_1 = \frac{16(\lambda+2\mu)}{3(3\lambda+4\mu)}\frac{1}{(1+M)}$$

$$U_3 = \frac{4(\lambda+2\mu)}{3(\lambda+\mu)}\frac{1}{(1+\kappa)}$$

where

$$M = \frac{4\mu'}{\pi\alpha\mu}\frac{(\lambda+2\mu)}{(3\lambda+4\mu)}$$

$$\kappa = \frac{[K'+(4/3)\mu'](\lambda+2\mu)}{\pi\alpha\mu(\lambda+\mu)}$$

with K' and μ' the bulk and shear modulus of the inclusion material. The criteria for an inclusion to be "weak" depend on its shape or aspect ratio α as well as on the relative moduli of the inclusion and matrix material. Dry cavities can be modeled by setting the inclusion moduli to zero. Fluid-saturated cavities are simulated by setting the inclusion shear modulus to zero.

CAUTION: Because the cavities are isolated with respect to flow, this approach simulates very-high-frequency behavior appropriate to ultrasonic laboratory conditions. At low frequencies, when there is time for wave-induced pore pressure increments to flow and equilibrate, it is better to find the effective moduli for dry cavities and then saturate them with the Brown and Korringa low-frequency relations. This should not be confused with the tendency to term this approach a low-frequency theory, for crack dimensions are assumed to be much smaller than a wavelength.

Hudson also gives expressions for infinitely thin fluid-filled cracks:

$$U_1 = \frac{16(\lambda+2\mu)}{3(3\lambda+4\mu)}$$

$$U_3 = 0$$

These assume no discontinuity in the normal component of crack displacements and therefore predict no change in the compressional modulus with saturation. There is, however, a shear displacement discontinuity and a resulting effect on shear stiffness. This case should be used with care.

The first-order changes λ_1 and μ_1 in the isotropic elastic moduli λ and μ of a material containing randomly oriented inclusions are given by

$$\mu_1 = -\frac{2\mu}{15}\varepsilon(3U_1+2U_3)$$

$$3\lambda_1 + 2\mu_1 = -\frac{(3\lambda+2\mu)^2}{3\mu}\varepsilon U_3$$

These results agree with the self-consistent results of Budiansky and O'Connell (1976).

For two or more crack sets aligned in different directions, corrections for each crack set are calculated separately in a crack-local coordinate system with the 3-axis normal to the crack plane and then rotated or transformed back (see Section 1.4 on coordinate transformations) into the coordinates of c_{ij}^{eff}; finally the results are added to get the overall correction. Thus, for three crack sets with crack densities ε_1, ε_2, and ε_3 with crack normals aligned along the 1-, 2- and 3-axis, respectively, the overall first-order corrections to c_{ij}^0, $c_{ij}^{1(3\text{sets})}$ may be given in terms of linear combinations of the corrections for a single set with the appropriate crack densities as follows (where we have taken into account the symmetry properties of c_{ij}^1):

$$c_{11}^{1(3\text{sets})} = c_{33}^1(\varepsilon_1) + c_{11}^1(\varepsilon_2) + c_{11}^1(\varepsilon_3)$$

$$c_{12}^{1(3\text{sets})} = c_{13}^1(\varepsilon_1) + c_{13}^1(\varepsilon_2) + c_{12}^1(\varepsilon_3)$$

$$c_{13}^{1(3\text{sets})} = c_{13}^{1}(\varepsilon_1) + c_{12}^{1}(\varepsilon_2) + c_{13}^{1}(\varepsilon_3)$$
$$c_{22}^{1(3\text{sets})} = c_{11}^{1}(\varepsilon_1) + c_{33}^{1}(\varepsilon_2) + c_{11}^{1}(\varepsilon_3)$$
$$c_{23}^{1(3\text{sets})} = c_{12}^{1}(\varepsilon_1) + c_{13}^{1}(\varepsilon_2) + c_{13}^{1}(\varepsilon_3)$$
$$c_{33}^{1(3\text{sets})} = c_{11}^{1}(\varepsilon_1) + c_{11}^{1}(\varepsilon_2) + c_{33}^{1}(\varepsilon_3)$$
$$c_{44}^{1(3\text{sets})} = c_{44}^{1}(\varepsilon_2) + c_{44}^{1}(\varepsilon_3)$$
$$c_{55}^{1(3\text{sets})} = c_{44}^{1}(\varepsilon_1) + c_{44}^{1}(\varepsilon_3)$$
$$c_{66}^{1(3\text{sets})} = c_{44}^{1}(\varepsilon_1) + c_{44}^{1}(\varepsilon_2)$$

Note that $c_{66}^{1} = 0$ and $c_{12}^{1} = c_{11}^{1} - 2c_{66}^{1} = c_{11}^{1}$.

Hudson (1981) also gives the attenuation coefficient ($\gamma = \omega Q^{-1}/2V$) for elastic waves in cracked media. For aligned cracks with normals along the 3-axis, the attenuation coefficients for P-, SV-, and SH-waves are

$$\gamma_P = \frac{\omega}{V_S}\varepsilon\left(\frac{\omega a}{V_P}\right)^3 \frac{1}{30\pi}\left[AU_1^2 \sin^2 2\theta + BU_3^2\left(\frac{V_P^2}{V_S^2} - 2\sin^2\theta\right)^2\right]$$

$$\gamma_{SV} = \frac{\omega}{V_S}\varepsilon\left(\frac{\omega a}{V_S}\right)^3 \frac{1}{30\pi}\left(AU_1^2 \cos^2 2\theta + BU_3^2 \sin^2 2\theta\right)$$

$$\gamma_{SH} = \frac{\omega}{V_S}\varepsilon\left(\frac{\omega a}{V_S}\right)^3 \frac{1}{30\pi}\left(AU_1^2 \cos^2\theta\right)$$

$$A = \frac{3}{2} + \frac{V_S^5}{V_P^5}$$

$$B = 2 + \frac{15}{4}\frac{V_S}{V_P} - 10\frac{V_S^3}{V_P^3} + 8\frac{V_S^5}{V_P^5}$$

In the preceding expressions V_P and V_S are the P and S velocities in the uncracked isotropic background matrix, ω is the angular frequency, and θ is the angle between the direction of propagation and the 3-axis (axis of symmetry).

For randomly oriented cracks (isotropic distribution), the P and S attenuation coefficients are given as

$$\gamma_P = \frac{\omega}{V_S}\varepsilon\left(\frac{\omega a}{V_P}\right)^3 \frac{4}{(15)^2\pi}\left[AU_1^2 + \frac{1}{2}\frac{V_P^5}{V_S^5}B(B-2)U_3^2\right]$$

$$\gamma_S = \frac{\omega}{V_S}\varepsilon\left(\frac{\omega a}{V_S}\right)^3 \frac{1}{75\pi}\left(AU_1^2 + \frac{1}{3}BU_3^2\right)$$

The fourth-power dependence on ω is characteristic of Rayleigh scattering.

Hudson (1990) gives results for overall elastic moduli of material with various distributions of penny-shaped cracks. If conditions at the cracks are taken to be

uniform so that U_1 and U_3 do not depend on the polar and azimuthal angles θ and ϕ, the first-order correction is given as

$$c_{ijpq}^{1} = -\frac{A}{\mu}U_3[\lambda^2\delta_{ij}\delta_{pq} + 2\lambda\mu(\delta_{ij}\tilde{\varepsilon}_{pq} + \delta_{pq}\tilde{\varepsilon}_{ij}) + 4\mu^2\tilde{\varepsilon}_{ijpq}]$$
$$- A\mu U_1(\delta_{jq}\tilde{\varepsilon}_{ip} + \delta_{jp}\tilde{\varepsilon}_{iq} + \delta_{iq}\tilde{\varepsilon}_{jp} + \delta_{ip}\tilde{\varepsilon}_{jq} - 4\tilde{\varepsilon}_{ijpq})$$

where

$$A = \int_0^{2\pi}\int_0^{\pi/2} \varepsilon(\theta,\phi)\sin\theta\, d\theta\, d\phi$$

$$\tilde{\varepsilon}_{ij} = \frac{1}{A}\int_0^{2\pi}\int_0^{\pi/2} \varepsilon(\theta,\phi)n_i n_j \sin\theta\, d\theta\, d\phi$$

$$\tilde{\varepsilon}_{ijpq} = \frac{1}{A}\int_0^{2\pi}\int_0^{\pi/2} \varepsilon(\theta,\phi)n_i n_j n_p n_q \sin\theta\, d\theta\, d\phi$$

and n_i are the components of the unit vector along the crack normal, $\boldsymbol{n} = (\sin\theta\cos\phi, \sin\theta\sin\phi, \cos\theta)$, whereas $\varepsilon(\theta,\phi)$ is the crack density distribution function so that $\varepsilon(\theta,\phi)\sin\theta\, d\theta\, d\phi$ is the density of cracks with normals lying in the solid angle between $(\theta, \theta + d\theta)$ and $(\phi, \phi + d\phi)$.

SPECIAL CASES OF CRACK DISTRIBUTIONS

a) When cracks with total crack density ε_t have all their normals aligned along $\theta = \theta_0, \phi = \phi_0$:

$$\varepsilon(\theta,\phi) = \varepsilon_t\frac{\delta(\theta-\theta_0)}{\sin\theta}\delta(\phi-\phi_0)$$

and then

$$A = \varepsilon_t$$
$$\tilde{\varepsilon}_{ij} = n_i^0 n_j^0$$
$$\tilde{\varepsilon}_{ijpq} = n_i^0 n_j^0 n_p^0 n_q^0$$

where $n_1^0 = \sin\theta_0\cos\phi_0$, $n_2^0 = \sin\theta_0\sin\phi_0$, $n_3^0 = \cos\theta_0$.

b) Rotationally symmetric crack distributions with normals symmetrically distributed about $\theta = 0$, that is, ε is a function of θ only:

$$A = 2\pi\int_0^{\pi/2}\varepsilon(\theta)\sin\theta\, d\theta$$
$$\tilde{\varepsilon}_{12} = \tilde{\varepsilon}_{23} = \tilde{\varepsilon}_{31} = 0$$
$$\tilde{\varepsilon}_{11} = \tilde{\varepsilon}_{22} = \frac{\pi}{A}\int_0^{\pi/2}\varepsilon(\theta)\sin^3\theta\, d\theta = \frac{1}{2}(1-\tilde{\varepsilon}_{33})$$

$$\tilde{\varepsilon}_{1111} = \tilde{\varepsilon}_{2222} = \frac{3\pi}{4A}\int_0^{\pi/2} \varepsilon(\theta)\sin^5\theta\, d\theta = 3\tilde{\varepsilon}_{1122} = 3\tilde{\varepsilon}_{1212}, \text{ etc.}$$

$$\tilde{\varepsilon}_{3333} = \frac{8}{3}\tilde{\varepsilon}_{1111} - 4\tilde{\varepsilon}_{11} + 1$$

$$\tilde{\varepsilon}_{1133} = \tilde{\varepsilon}_{11} - \frac{4}{3}\tilde{\varepsilon}_{1111} = \tilde{\varepsilon}_{2233} = \tilde{\varepsilon}_{1313} = \tilde{\varepsilon}_{2323}, \text{ etc.}$$

Elements other than those related to the preceding elements by symmetry are zero. A particular rotationally symmetric distribution is the Fisher distribution, for which $\varepsilon(\theta)$ is

$$\varepsilon(\theta) = \frac{\varepsilon_t}{2\pi}\frac{e^{(\cos\theta)/\sigma^2}}{\sigma^2\left(e^{1/\sigma^2}-1\right)}$$

For small σ^2, this is approximately a model for a Gaussian distribution on the sphere

$$\varepsilon(\theta) \approx \varepsilon_t \frac{e^{-\theta^2/2\sigma^2}}{2\pi\sigma^2}$$

The proportion of crack normals outside the range $0 \le \theta \le 2\sigma$ is approximately $1/e^2$. For this distribution,

$$A = \varepsilon_t$$

$$\tilde{\varepsilon}_{11} = \frac{-1 + 2\sigma^2 e^{1/\sigma^2} - 2\sigma^4\left(e^{1/\sigma^2}-1\right)}{2\left(e^{1/\sigma^2}-1\right)} \approx \sigma^2$$

$$\tilde{\varepsilon}_{1111} = \frac{3}{8}\left[\frac{-1 + 4\sigma^4\left(2e^{1/\sigma^2}+1\right) - 24\sigma^6 e^{1/\sigma^2} + 24\sigma^8\left(e^{1/\sigma^2}-1\right)}{\left(e^{1/\sigma^2}-1\right)}\right] \approx 3\sigma^4$$

This distribution is suitable when crack normals are oriented randomly with a small variance about a mean direction along the 3-axis.

c) Cracks with normals randomly distributed at a fixed angle from the 3-axis forming a cone. In this case ε is independent of ϕ and is zero unless $\theta = \theta_0, 0 \le \phi \le 2\pi$.

$$\varepsilon(\theta) = \varepsilon_t \frac{\delta(\theta - \theta_0)}{2\pi\sin\theta}$$

which gives

$$A = \varepsilon_t$$

$$\tilde{\varepsilon}_{11} = \frac{1}{2}\sin^2\theta_0$$

$$\tilde{\varepsilon}_{1111} = \frac{3}{8}\sin^4\theta_0$$

and the first-order corrections are

$$c^1_{1111} = \frac{-\varepsilon_t}{2\mu}[U_3(2\lambda^2 + 4\lambda\mu\sin^2\theta_0 + 3\mu^2\sin^4\theta_0) + U_1\mu^2\sin^2\theta_0(4 - 3\sin^2\theta_0)]$$

$$= c^1_{2222}$$

$$c^1_{3333} = \frac{-\varepsilon_t}{\mu}[U_3(\lambda + 2\mu\cos^2\theta_0)^2 + U_1\mu^2 4\cos^2\theta_0\sin^2\theta_0]$$

$$c^1_{1122} = \frac{-\varepsilon_t}{2\mu}[U_3(2\lambda^2 + 4\lambda\mu\sin^2\theta_0 + \mu^2\sin^4\theta_0) - U_1\mu^2\sin^4\theta_0]$$

$$c^1_{1133} = \frac{-\varepsilon_t}{\mu}[U_3(\lambda + \mu\sin^2\theta_0)(\lambda + 2\mu\cos^2\theta_0) - U_1\mu^2 2\sin^2\theta_0\cos^2\theta_0]$$

$$= c^1_{2233}$$

$$c^1_{2323} = \frac{-\varepsilon_t}{2}\mu[U_3 4\sin^2\theta_0\cos^2\theta_0 + U_1(\sin^2\theta_0 + 2\cos^2\theta_0 - 4\sin^2\theta_0\cos^2\theta_0)]$$

$$= c^1_{1313}$$

$$c^1_{1212} = \frac{-\varepsilon_t}{2}\mu[U_3\sin^4\theta_0 + U_1\sin^2\theta_0(2 - \sin^2\theta_0)]$$

USES

Hudson's model is used to estimate the effective elastic moduli and attenuation of a rock in terms of its constituents and pore space.

ASSUMPTIONS AND LIMITATIONS

The use of Hudson's model requires the following considerations:

- Idealized crack shape (penny-shaped) with small aspect ratios and crack density are assumed. Crack radius and distance between cracks are much smaller than a wavelength. The formal limit quoted by Hudson for both first- and second-order terms is ε less than 0.1.
- The second-order expansion is not a uniformly converging series and predicts increasing moduli with crack density beyond the formal limit (Cheng, 1993). Better results will be obtained by using just the first-order correction rather than inappropriately using the second-order correction. Cheng gives a new expansion based on Padé approximation, which avoids this problem.
- Cracks are isolated with respect to fluid flow. Pore pressures are unequilibrated and adiabatic. The model is appropriate for high-frequency laboratory conditions. For low-frequency field situations use Hudson's dry equations and

then saturate by using Brown and Korringa relations. This should not be confused with the tendency to think of this approach as a low-frequency theory, because crack dimensions are assumed to be much smaller than a wavelength.

- Sometimes a single crack set may not be an adequate representation of crack-induced anisotropy. In this case we need to superpose several crack sets with angular distributions.

4.11 ESHELBY-CHENG MODEL FOR CRACKED ANISOTROPIC MEDIA

SYNOPSIS

Cheng (1978, 1993) has given a model for the effective moduli of cracked transversely isotropic rocks based on Eshelby's (1957) static solution for the strain inside an ellipsoidal inclusion in an isotropic matrix. The effective moduli c_{ij}^{eff} for a rock containing fluid-filled ellipsoidal cracks with their normals aligned along the 3-axis are given as

$$c_{ij}^{\text{eff}} = c_{ij}^{0} - \phi c_{ij}^{1}$$

where ϕ is the porosity and c_{ij}^{0} are the moduli of the uncracked isotropic rock. The corrections c_{ij}^{1} are

$$c_{11}^{1} = \lambda(S_{31} - S_{33} + 1) + \frac{2\mu E}{D(S_{12} - S_{11} + 1)}$$

$$c_{33}^{1} = \frac{(\lambda + 2\mu)(-S_{12} - S_{11} + 1) + 2\lambda S_{13} + 4\mu C}{D}$$

$$c_{13}^{1} = \frac{(\lambda + 2\mu)(S_{13} + S_{31}) - 4\mu C + \lambda(S_{13} - S_{12} - S_{11} - S_{33} + 2)}{2D}$$

$$c_{44}^{1} = \frac{\mu}{1 - 2S_{1313}}$$

$$c_{66}^{1} = \frac{\mu}{1 - 2S_{1212}}$$

with

$$C = \frac{K_{\text{fl}}}{3(K - K_{\text{fl}})}$$

$$D = S_{33}S_{11} + S_{33}S_{12} - 2S_{31}S_{13} - (S_{11} + S_{12} + S_{33} - 1 - 3C) - C[S_{11} + S_{12} + 2(S_{33} - S_{13} - S_{31})]$$

$$E = S_{33}S_{11} - S_{31}S_{13} - (S_{33} + S_{11} - 2C - 1) + C(S_{31} + S_{13} - S_{11} - S_{33})$$

$$S_{11} = QI_{aa} + RI_a$$

$$S_{33} = Q\left(\frac{4\pi}{3} - 2I_{ac}\alpha^2\right) + I_cR$$

$$S_{12} = QI_{ab} - RI_a$$

$$S_{13} = QI_{ac}\alpha^2 - RI_a$$

$$S_{31} = QI_{ac} - RI_c$$

$$S_{1212} = QI_{ab} + RI_a$$

$$S_{1313} = \frac{Q(1 + \alpha^2)I_{ac}}{2} + \frac{R(I_a + I_c)}{2}$$

$$I_a = \frac{2\pi\alpha(\cos^{-1}\alpha - \alpha S_a)}{S_a^3}$$

$$I_c = 4\pi - 2I_a$$

$$I_{ac} = \frac{I_c - I_a}{3S_a^2}$$

$$I_{aa} = \pi - \frac{3I_{ac}}{4}$$

$$I_{ab} = \frac{I_{aa}}{3}$$

$$\sigma = \frac{3K - 2\mu}{6K + 2\mu}$$

$$S_a = \sqrt{1 - \alpha^2}$$

$$R = \frac{1 - 2\sigma}{8\pi(1 - \sigma)}$$

$$Q = \frac{3R}{1 - 2\sigma}$$

In the preceding equations K and μ are the bulk and shear modulus of the isotropic matrix, respectively; K_{fl} is the bulk modulus of the fluid; and α is the crack aspect ratio. Dry cavities can be modeled by setting the inclusion moduli to zero. Do not confuse the S's with the anisotropic compliance tensor. This model is valid for arbitrary aspect ratios, unlike the Hudson model (see Section 4.10 on Hudson's model), which assumes very small aspect ratio cracks. The results of the

two models are essentially the same for small aspect ratios and low crack densities (<0.1) as long as the "weak inclusion" form of Hudson's theory is used (Cheng, 1993).

USES

The Eshelby–Cheng model is used to obtain effective anisotropic stiffness tensor for transversely isotropic cracked rocks.

ASSUMPTIONS AND LIMITATIONS

The following presuppositions and limitations apply to the Eshelby–Cheng model:

- The model assumes an isotropic, homogeneous, elastic background matrix and an idealized ellipsoidal crack shape.
- The model assumes low crack concentrations but can handle all aspect ratios.
- Because the cavities are isolated with respect to flow, this approach simulates very-high-frequency behavior appropriate to ultrasonic laboratory conditions. At low frequencies, when there is time for wave-induced pore pressure increments to flow and equilibrate, it is better to find the effective moduli for dry cavities and then saturate them with the Brown and Korringa low-frequency relations. This should not be confused with the tendency to term this approach a low-frequency theory, for crack dimensions are assumed to be much smaller than a wavelength.

EXTENSIONS

The model has been extended to a transversely isotropic background by Nishizawa (1982).

4.12 ELASTIC CONSTANTS IN FINELY LAYERED MEDIA – BACKUS AVERAGE

SYNOPSIS

A transversely isotropic medium with the symmetry axis in the x_3 direction has an elastic stiffness tensor that can be written in the condensed matrix form (see

Section 2.2 on anisotropy):

$$\begin{bmatrix} a & b & f & 0 & 0 & 0 \\ b & a & f & 0 & 0 & 0 \\ f & f & c & 0 & 0 & 0 \\ 0 & 0 & 0 & d & 0 & 0 \\ 0 & 0 & 0 & 0 & d & 0 \\ 0 & 0 & 0 & 0 & 0 & m \end{bmatrix}, \quad m = \frac{1}{2}(a-b)$$

where a, b, c, d, and f are five independent elastic constants. Backus (1962) showed that in the long-wavelength limit a stratified medium composed of **layers of transversely isotropic materials** (each with its symmetry axis normal to the strata) is also effectively anisotropic with effective stiffness as follows:

$$\begin{bmatrix} A & B & F & 0 & 0 & 0 \\ B & A & F & 0 & 0 & 0 \\ F & F & C & 0 & 0 & 0 \\ 0 & 0 & 0 & D & 0 & 0 \\ 0 & 0 & 0 & 0 & D & 0 \\ 0 & 0 & 0 & 0 & 0 & M \end{bmatrix}, \quad M = \frac{1}{2}(A-B)$$

where

$$A = \langle a - f^2 c^{-1} \rangle + \langle c^{-1} \rangle^{-1} \langle f c^{-1} \rangle^2$$
$$B = \langle b - f^2 c^{-1} \rangle + \langle c^{-1} \rangle^{-1} \langle f c^{-1} \rangle^2$$
$$C = \langle c^{-1} \rangle^{-1}$$
$$F = \langle c^{-1} \rangle^{-1} \langle f c^{-1} \rangle$$
$$D = \langle d^{-1} \rangle^{-1}$$
$$M = \langle m \rangle$$

The brackets $\langle \cdot \rangle$ indicate averages of the enclosed properties weighted by their volumetric proportions. This is often called the *Backus average*.

If the **individual layers are isotropic**, the effective medium is still transversely isotropic, but the number of independent constants needed to describe each individual layer is reduced to 2:

$$a = c = \lambda + 2\mu, \quad b = f = \lambda, \quad d = m = \mu$$

giving for the effective medium

$$A = \left\langle \frac{4\mu(\lambda+\mu)}{\lambda+2\mu} \right\rangle + \left\langle \frac{1}{\lambda+2\mu} \right\rangle^{-1} \left\langle \frac{\lambda}{\lambda+2\mu} \right\rangle^2$$
$$B = \left\langle \frac{2\mu\lambda}{\lambda+2\mu} \right\rangle + \left\langle \frac{1}{\lambda+2\mu} \right\rangle^{-1} \left\langle \frac{\lambda}{\lambda+2\mu} \right\rangle^2$$

$$C = \left\langle \frac{1}{\lambda + 2\mu} \right\rangle^{-1}$$

$$F = \left\langle \frac{1}{\lambda + 2\mu} \right\rangle^{-1} \left\langle \frac{\lambda}{\lambda + 2\mu} \right\rangle$$

$$D = \left\langle \frac{1}{\mu} \right\rangle^{-1}$$

$$M = \langle \mu \rangle$$

In terms of the P- and S-wave velocities and densities in the isotropic layers (Levin, 1979),

$$a = \rho V_P^2$$

$$d = \rho V_S^2$$

$$f = \rho(V_P^2 - V_S^2)$$

the effective parameters can be rewritten as

$$A = \left\langle 4\rho V_S^2 \left[1 - \frac{V_S^2}{V_P^2} \right] \right\rangle + \left\langle 1 - 2\frac{V_S^2}{V_P^2} \right\rangle^2 \langle (\rho V_P^2)^{-1} \rangle^{-1}$$

$$B = \left\langle 2\rho V_S^2 \left[1 - \frac{2V_S^2}{V_P^2} \right] \right\rangle + \left\langle 1 - 2\frac{V_S^2}{V_P^2} \right\rangle^2 \langle (\rho V_P^2)^{-1} \rangle^{-1}$$

$$C = \langle (\rho V_P^2)^{-1} \rangle^{-1}$$

$$F = \left\langle 1 - 2\frac{V_S^2}{V_P^2} \right\rangle \langle (\rho V_P^2)^{-1} \rangle^{-1}$$

$$D = \langle (\rho V_S^2)^{-1} \rangle^{-1}$$

$$M = \langle \rho V_S^2 \rangle$$

The P- and S-wave velocities in the effective anisotropic medium can be written as

$$V_{SH,h} = \sqrt{M/\rho}$$

$$V_{SH,v} = V_{SV,h} = V_{SV,v} = \sqrt{D/\rho}$$

$$V_{P,h} = \sqrt{A/\rho}$$

$$V_{P,v} = \sqrt{C/\rho}$$

where ρ is the average density; $V_{P,v}$ is the vertically propagating P wave; $V_{P,h}$ is the horizontally propagating P wave; $V_{SH,h}$ is the horizontally propagating, horizontally polarized S wave; $V_{SV,h}$ is the horizontally propagating, vertically polarized S wave; and $V_{SV,v}$ and $V_{SH,v}$ are the vertically propagating S waves of any polarization (vertical is defined as normal to the layering).

EXAMPLE

Calculate the effective anisotropic elastic constants and the velocity anisotropy for a thinly layered sequence of dolomite and shale with the following layer properties:

$V_{P(1)} = 5{,}200$ m/s, $V_{S(1)} = 2{,}700$ m/s, $\rho_1 = 2{,}450$ kg/m^3, $d_1 = 0.75$ m

$V_{P(2)} = 2{,}900$ m/s, $V_{S(2)} = 1{,}400$ m/s, $\rho_2 = 2{,}340$ kg/m^3, $d_2 = 0.5$ m

The volumetric fractions are

$$f_1 = d_1/(d_1 + d_2) = 0.6, \quad f_2 = d_2/(d_1 + d_2) = 0.4$$

If one takes the volumetric weighted averages of the appropriate properties,

$$A = f_1 4\rho_1 V_{S(1)}^2 \left(1 - \frac{V_{S(1)}^2}{V_{P(1)}^2} \right) + f_2 4\rho_2 V_{S(2)}^2 \left(1 - \frac{V_{S(2)}^2}{V_{P(2)}^2} \right)$$

$$+ \left[f_1 \left(1 - 2\frac{V_{S(1)}^2}{V_{P(1)}^2} \right) + f_2 \left(1 - 2\frac{V_{S(2)}^2}{V_{P(2)}^2} \right) \right]^2 \frac{1}{\dfrac{f_1}{\rho_1 V_{P(1)}^2} + \dfrac{f_2}{\rho_2 V_{P(2)}^2}}$$

$A = 45.1$ GPa

Similarly, computing the other averages we get

$C = 34.03$ GPa, $D = 8.28$ GPa, $M = 12.55$ GPa, $F = 16.7$ GPa

$B = A - 2M = 20$ GPa

The average density $\rho = f_1\rho_1 + f_2\rho_2 = 2{,}406$ kg/m^3. The anisotropic velocities are

$$V_{SH,h} = \sqrt{M/\rho} = 2{,}284.0 \text{ m/s}$$

$$V_{SH,v} = V_{SV,h} = V_{SV,v} = \sqrt{D/\rho} = 1{,}854.8$$

$$V_{P,h} = \sqrt{A/\rho} = 4{,}329.5 \text{ m/s}$$

$$V_{P,v} = \sqrt{C/\rho} = 3{,}761.0 \text{ m/s}$$

P-wave anisotropy $= (4{,}329.5 - 3{,}761.0)/3{,}761.0 \approx 15\%$

S-wave anisotropy $= (2{,}284.0 - 1{,}854.8)/1{,}854.8 \approx 23\%$

Finally, consider the case in which **each layer is isotropic with the same shear modulus** but with a different bulk modulus. This might be the situation, for example, for a massive, homogeneous rock with fine layers of different fluids or saturations. Then, the elastic constants of the medium become

$$A = C = \left\langle \frac{1}{\rho V_P{}^2} \right\rangle^{-1} = \left\langle \frac{1}{K + \frac{4}{3}\mu} \right\rangle^{-1}$$

$$B = F = \left\langle \frac{1}{\rho V_P{}^2} \right\rangle^{-1} - 2\mu = \left\langle \frac{1}{K + \frac{4}{3}\mu} \right\rangle^{-1} - 2\mu = A - 2\mu$$

$$D = M = \mu$$

A finely layered medium of isotropic layers, all having the same shear modulus, is isotropic.

USES

The Backus average is used to model a finely stratified medium as a single homogeneous medium.

ASSUMPTIONS AND LIMITATIONS

The following presuppositions and conditions apply to the Backus average:

- All materials are linear elastic.
- There are no sources of intrinsic energy dissipation such as friction or viscosity.
- Layer thickness must be much smaller than the seismic wavelength. How small is still a question of disagreement and research, but a rule of thumb is that the wavelength must be at least ten times the layer thickness.

PART 5

GRANULAR MEDIA

5.1 PACKING OF SPHERES — GEOMETRIC RELATIONS

SYNOPSIS

Spheres are often used as idealized models for pores or grains. Table 5.1.1 gives some geometric properties of various packings of identical spheres (summarized in part from Bourbié et al., 1987). Note that complementary interpretations are possible when the grains are considered spheres versus when the pores are considered spheres.

USES

These results can be used to estimate the geometric relations of the packing of granular materials.

ASSUMPTIONS AND LIMITATIONS

The preceding results assume idealized, identical spheres.

TABLE 5.1.1. Geometric properties of sphere packs.

Packing type	Porosity (nonspheres)	Solid fraction (spheres)	Specific surface area[a]	Number of contacts per sphere	Radius of maximum inscribable sphere[b,c]	Radius of maximum sphere fitting in narrowest channels[b,c]
Simple cubic	$1-\pi/6=0.476$	$\pi/6=0.524$	$\pi/2R$	6	0.732	0.414
Simple hexagonal	$1-4\pi\cos(\pi/6)/18=0.395$	$4\pi\cos(\pi/6)/18=0.605$	$2\pi\cos(\pi/6)/3R$	8	0.528	0.414 and 0.155
Hexagonal close pack	0.259	0.741	$2.22/R$	12	0.225 and 0.414	0.155
Dense random pack	~0.36	~0.64	$\sim 1.92/R$	~9		

[a]Specific surface area, S, is defined as the pore surface area in a sample divided by the total volume of the sample. If the grains are spherical, $S=3(1-\phi)/R$.
[b]Expressed in units of the radius of the packed spheres.
[c]Note that if the pore space is modeled as a packing of spherical pores, the inscribable spheres always have radius equal to 1.

5.2 RANDOM SPHERICAL GRAIN PACKINGS – CONTACT MODELS AND EFFECTIVE MODULI

SYNOPSIS

CONTACT STIFFNESSES AND EFFECTIVE MODULI

The effective elastic properties of packings of spherical particles depend on *normal and tangential contact stiffnesses of a two-particle combination*. The normal stiffness of two identical spheres is defined as the ratio of a confining force increment to the shortening of a sphere radius. The tangential stiffness of two identical spheres is the ratio of a tangential force increment to the increment of the tangential displacement of the center relative to the contact region:

$$S_n = \partial F/\partial\delta, \quad S_\tau = \partial T/\partial\tau$$

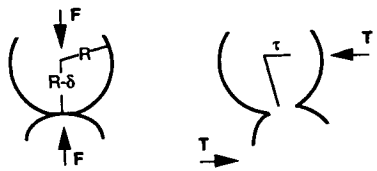

Figure 5.2.1

For a random sphere packing, effective bulk and shear moduli can be expressed through porosity, ϕ; coordination number, C (the average number of contacts per sphere); sphere radius, R; and normal and tangential stiffnesses, S_n and S_τ, respectively, of a two-sphere combination by

$$K_{\text{eff}} = \frac{C(1-\phi)}{12\pi R} S_n$$

$$G_{\text{eff}} = \frac{C(1-\phi)}{20\pi R}(S_n + 1.5S_\tau)$$

The effective P- and S-wave velocities are (Winkler, 1983)

$$V_P^2 = \frac{3C}{20\pi R\rho}\left(S_n + \frac{2}{3}S_\tau\right)$$

$$V_S^2 = \frac{C}{20\pi R\rho}\left(S_n + \frac{3}{2}S_\tau\right)$$

$$\frac{V_P^2}{V_S^2} = 2\frac{3S_n/S_\tau + 2}{2S_n/S_\tau + 3}$$

where ρ is the grain-material density. Wang and Nur (1992) summarize some of the existing granular media models.

COORDINATION NUMBER

For a random dense pack of identical spheres the average number of contacts per grain C is about 9. An approximate C versus porosity curve, shown in Figure 5.2.2, is based on the summary in Murphy (1982).

THE HERTZ–MINDLIN MODEL

In the **Hertz model** of normal compression of two identical spheres, the radius of the contact area, a, and the normal displacement, δ, are

$$a = \sqrt[3]{\frac{3FR}{8G}(1-\nu)}, \quad \delta = \frac{a^2}{R}$$

where G and ν are the shear modulus and Poisson's ratio of the grain material, respectively.

If a hydrostatic confining pressure P is applied to a random identical sphere packing, a confining force acting between two particles is

$$F = \frac{4\pi R^2 P}{C(1-\phi)}$$

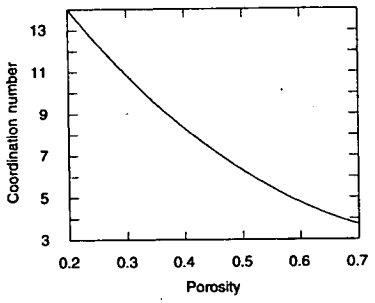

Porosity	C
0.20	14.007
0.25	12.336
0.30	10.843
0.35	9.5078
0.40	8.3147
0.45	7.2517
0.50	6.3108
0.55	5.4878
0.60	4.7826
0.65	4.1988
0.7	3.7440

Figure 5.2.2

Then

$$a = R\sqrt[3]{\frac{3\pi(1-\nu)}{2C(1-\phi)G}P}$$

The normal stiffness is

$$S_n = \frac{4Ga}{1-\nu}$$

The effective bulk modulus of a dry random identical sphere packing is, then,

$$K_{eff} = \sqrt[3]{\frac{C^2(1-\phi)^2G^2}{18\pi^2(1-\nu)^2}P}$$

Mindlin (1949) shows that if the spheres are first pressed together and a tangential force is applied *afterward*, the shear and normal stiffnesses are (the latter as in the Hertz solution)

$$S_\tau = \frac{8aG}{2-\nu}, \quad S_n = \frac{4aG}{1-\nu}$$

where ν and G are the Poisson's ratio and shear modulus of the solid grains, respectively. The effective shear modulus of a dry random identical sphere packing is, then,

$$G_{eff} = \frac{5-4\nu}{5(2-\nu)}\sqrt[3]{\frac{3C^2(1-\phi)^2G^2}{2\pi^2(1-\nu)^2}P}$$

In the Mindlin formulas given above, it is assumed that there is no slip at the contact surface between two particles. In fact such slip will occur at the edges of the contact region. The no-slip assumption results in a small error if only acoustic wave propagation is concerned and can be safely used in estimating the effective moduli of granular materials. *The Hertz–Mindlin model can be used to describe the properties of precompacted granular rocks.*

THE WALTON MODEL

It is assumed in the Walton model (Walton, 1987) that *normal and shear deformation of a two-grain combination occur simultaneously*. This assumption leads to results somewhat different from those given by the Hertz–Mindlin model. Specifically, there is no partial slip in the contact area. The slip occurs across the whole area once applied tractions exceed friction resistance. The results discussed in the following paragraphs are given for two special cases: infinitely rough spheres (friction coefficient is very large) and ideally smooth spheres (friction coefficient is zero).

Under *hydrostatic pressure* P, an identical sphere packing is isotropic. Its effective bulk and shear moduli for the rough spheres case (dry pack) are described

by

$$K_{\text{eff}} = \frac{1}{6}\sqrt[3]{\frac{3(1-\phi)^2C^2P}{\pi^4B^2}}, \quad G_{\text{eff}} = \frac{3}{5}K_{\text{eff}}\frac{5B+A}{2B+A}$$

$$A = \frac{1}{4\pi}\left(\frac{1}{G} - \frac{1}{G+\lambda}\right), \quad B = \frac{1}{4\pi}\left(\frac{1}{G} + \frac{1}{G+\lambda}\right)$$

where λ is Lamé's coefficient of the grain material. For the smooth spheres case (dry pack)

$$G_{\text{eff}} = \frac{1}{10}\sqrt[3]{\frac{3(1-\phi)^2C^2P}{\pi^4B^2}}, \quad K_{\text{eff}} = \frac{5}{3}G_{\text{eff}}$$

It is clear that the effective density of the aggregate is

$$\rho_{\text{eff}} = (1-\phi)\rho$$

Under *uniaxial pressure* σ_1 a dry identical sphere packing is transversely isotropic, and if the spheres are infinitely rough, it can be described by the following five constants:

$$C_{11} = 3(\alpha + 2\beta), \quad C_{12} = \alpha - 2\beta, \quad C_{13} = 2C_{12}$$

$$C_{33} = 8(\alpha + \beta), \quad C_{44} = \alpha + 7\beta$$

where

$$\alpha = \frac{(1-\phi)Ce}{32\pi^2B}, \quad \beta = \frac{(1-\phi)Ce}{32\pi^2(2B+A)}$$

$$e = \sqrt[3]{\frac{24\pi^2B(2B+A)\sigma_1}{(1-\phi)AC}}$$

THE DIGBY MODEL

The Digby model gives effective moduli for a dry random packing of identical elastic spherical particles. Neighboring particles are initially firmly bonded across small, flat, circular regions of the radius a. Outside these adhesion surfaces, the shape of each particle is assumed to be ideally smooth (with a continuous first derivative). Notice that this condition differs from that of Hertz, where the shape of a particle is not smooth at the intersection of the spherical surface and the plane of contact. Digby's normal and shear stiffnesses under hydrostatic pressure P are (Digby, 1981)

$$S_n = \frac{4Gb}{1-\nu}, \quad S_\tau = \frac{8Ga}{2-\nu}$$

where ν and G are the Poisson's ratio and shear modulus of the grain material respectively. Parameter b can be found from the relation

$$\frac{b}{R} = \left[(d)^2 + \left(\frac{a}{R}\right)^2\right]^{1/2}$$

where d satisfies the cubic equation

$$d^3 + \frac{3}{2}\left(\frac{a}{R}\right)^2 d - \frac{3\pi(1-\nu)}{2C(1-\phi)}\frac{P}{G} = 0$$

EXAMPLE

Use the Digby model to estimate the effective bulk and shear moduli for a dry random pack of spherical grains under a confining pressure of 10 MPa. The ratio of the radius of the initially bonded area to the grain radius a/R is 0.01. The bulk and shear moduli of the grain material are $K = 37$ GPa and $G = 44$ GPa, respectively. The porosity of the grain pack is 0.36.

The Poisson's ratio ν for the grain material is calculated from K and G:

$$\nu = \frac{3K - 2G}{2(3K + G)} = 0.07$$

The coordination number $C = 9$. Solving the cubic equation for d

$$d^3 + \frac{3}{2}\left(\frac{a}{R}\right)^2 d - \frac{3\pi(1-\nu)}{2C(1-\phi)}\frac{P}{G} = 0$$

and taking the real root, neglecting the pair of complex conjugate roots, we get $d = 0.0547$. Next we calculate b/R as

$$b/R = \sqrt{d^2 + \left(\frac{a}{R}\right)^2} = 0.0556$$

The values of a/R and b/R are used to compute S_n/R and S_τ/R:

$$S_n/R = \frac{4G(b/R)}{1-\nu} = 10.5, \quad S_\tau/R = \frac{8G(a/R)}{2-\nu} = 1.8$$

which then finally give us

$$K_{\text{eff}} = \frac{C(1-\phi)}{12\pi}(S_n/R) = 1.6\ \text{GPa}$$

and

$$G_{\text{eff}} = \frac{C(1-\phi)}{20\pi}[(S_n/R) + 1.5(S_\tau/R)] = 1.2\ \text{GPa}$$

THE BRANDT MODEL

The Brandt model allows one to calculate the bulk modulus of randomly packed elastic spheres of identical mechanical properties but of different sizes. This packing is subject to external hydrostatic and internal hydrostatic pressures. The effective pressure P is the difference between these two pressures. The effective bulk modulus is (Brandt, 1955)

$$K_{\text{eff}} = \frac{2P^{1/3}}{9\phi}\left[\frac{E}{1.75(1-\nu^2)}\right]^{2/3} Z - 1.5PZ$$

$$Z = \frac{(1+30.75z)^{5/3}}{1+46.13z}, \quad z = \frac{K^{3/2}(1-\nu^2)}{E\sqrt{P}}$$

In this case E is the mineral Young's modulus, and K is the fluid bulk modulus.

THE CEMENTED SAND MODEL

The cemented sand model allows one to calculate the bulk and shear moduli of dry sand in which cement is deposited *at grain contacts*. The cement is elastic and its properties may differ from those of the spheres.

It is assumed that the starting framework of cemented sand is a dense, random pack of identical spherical grains with porosity $\phi_0 \approx 0.36$ and the average number of contacts per grain $C = 9$. Adding cement to the grains acts to reduce porosity and to increase the effective elastic moduli of the aggregate. Then, these effective dry-rock bulk and shear moduli are (Dvorkin and Nur, 1996)

$$K_{\text{eff}} = \frac{1}{6}C(1-\phi_0)M_c\hat{S}_n$$

$$G_{\text{eff}} = \frac{3}{5}K_{\text{eff}} + \frac{3}{20}C(1-\phi_0)G_c\hat{S}_\tau$$

$$M_c = \rho_c V_{Pc}{}^2$$

$$G_c = \rho_c V_{Sc}{}^2$$

where ρ_c is the cement's density and V_{Pc} and V_{Sc} are its P- and S-wave velocities. Parameters $\hat{S}_n$ and $\hat{S}_\tau$ are proportional to the normal and shear stiffness, respectively, of a cemented two-grain combination. They depend on the amount of the contact cement and on the properties of the cement and the grains as defined in the following relations:

$$\hat{S}_n = A_n\alpha^2 + B_n\alpha + C_n$$

$$A_n = -0.024153\Lambda_n^{-1.3646}$$

$$B_n = 0.20405\Lambda_n^{-0.89008}$$

$$C_n = 0.00024649\Lambda_n^{-1.9864}$$

$$\hat{S}_\tau = A_\tau\alpha^2 + B_\tau\alpha + C_\tau$$

$$A_\tau = -10^{-2}(2.26\nu^2 + 2.07\nu + 2.3)\Lambda_\tau^{0.079\nu^2+0.1754\nu-1.342}$$

$$B_\tau = (0.0573\nu^2 + 0.0937\nu + 0.202)\Lambda_\tau^{0.0274\nu^2+0.0529\nu-0.8765}$$

$$C_\tau = -10^{-4}(9.654\nu^2 + 4.945\nu + 3.1)\Lambda_\tau^{0.01867\nu^2+0.4011\nu-1.8186}$$

$$\Lambda_n = \frac{2G_c}{\pi G}\frac{(1-\nu)(1-\nu_c)}{(1-2\nu_c)}, \quad \Lambda_\tau = \frac{G_c}{\pi G}, \quad \alpha = \frac{a}{R}$$

where G and ν are the shear modulus and the Poisson's ratio of the grains, respectively; G_c and ν_c are the shear modulus and the Poisson's ratio of the cement, respectively; a is the radius of the contact cement layer; and R is the grain radius.

The amount of the contact cement can be expressed through the ratio α of the radius of the cement layer a to the grain radius R:

$$\alpha = a/R$$

The radius of the contact cement layer a is not necessarily directly related to the total amount of cement; part of the cement may be deposited away from the intergranular contacts. However, by assuming that porosity reduction in sands is due to cementation only and by adopting certain schemes of cement deposition, we can relate parameter α to the current porosity of cemented sand ϕ. For example, we can use Scheme 1 (see Figure 5.2.3 below) in which all cement is deposited at grain contacts to get the formula

$$\alpha = 2\left[\frac{\phi_0 - \phi}{3C(1-\phi_0)}\right]^{0.25} = 2\left[\frac{S\phi_0}{3C(1-\phi_0)}\right]^{0.25}$$

or we can use Scheme 2 in which cement is evenly deposited on the grain surface:

$$\alpha = \left[\frac{2(\phi_0 - \phi)}{3(1-\phi_0)}\right]^{0.5} = \left[\frac{2S\phi_0}{3(1-\phi_0)}\right]^{0.5}$$

In these formulas S is the cement saturation of the pore space. It is the fraction of the pore space (of the uncemented sand) occupied by cement (in the cemented sand).

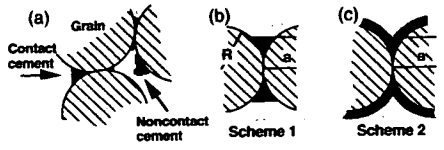

Figure 5.2.3

If the cement's properties are identical to those of the grains, the cementation theory gives results that are very close to those of the Digby model. The cementation theory allows one to **diagnose** a rock by determining what type of cement prevails. For example, the theory helps to distinguish between quartz and clay cement. Generally, V_P predictions are much better than V_S predictions.

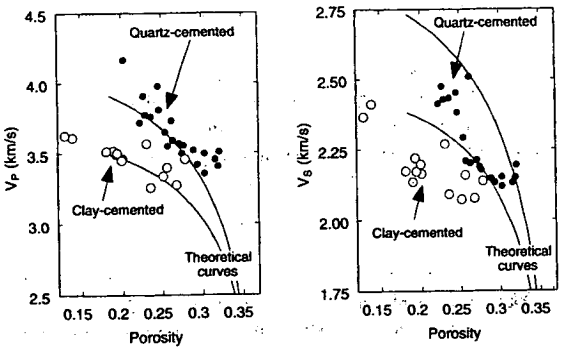

Figure 5.2.4. Predictions of V_P and V_S using the Scheme 2 model for quartz and clay cement compared with data from quartz and clay cemented rocks from the North Sea.

THE UNCEMENTED SAND MODEL

The uncemented sand model allows one to calculate the bulk and shear moduli of dry sand in which cement is deposited *away from grain contacts*. It is assumed that the starting framework of uncemented sand is a dense random pack of identical spherical grains with porosity $\phi_0 = 0.36$ and the average number of contacts per grain $C = 9$. At this porosity, the contact Hertz–Mindlin theory gives the following expressions for the effective bulk (K_{HM}) and shear (G_{HM}) moduli of a dry dense random pack of identical spherical grains subject to a hydrostatic pressure P:

$$K_{HM} = \left[\frac{C^2(1-\phi_0)^2G^2}{18\pi^2(1-\nu)^2}P\right]^{1/3}$$

$$G_{HM} = \frac{5-4\nu}{5(2-\nu)}\left[\frac{3C^2(1-\phi_0)^2G^2}{2\pi^2(1-\nu)^2}P\right]^{1/3}$$

where ν is the grain Poisson's ratio and G is the grain shear modulus.

To find the effective moduli (K_{eff} and G_{eff}) at a different porosity ϕ, a heuristic modified Hashin–Strikman lower bound is used:

$$K_{eff} = \left[\frac{\phi/\phi_0}{K_{HM}+\frac{4}{3}G_{HM}} + \frac{1-\phi/\phi_0}{K+\frac{4}{3}G_{HM}}\right]^{-1} - \frac{4}{3}G_{HM}$$

$$G_{eff} = \left[\frac{\phi/\phi_0}{G_{HM}+\frac{G_{HM}}{6}\left(\frac{9K_{HM}+8G_{HM}}{K_{HM}+2G_{HM}}\right)} + \frac{1-\phi/\phi_0}{G+\frac{G_{HM}}{6}\left(\frac{9K_{HM}+8G_{HM}}{K_{HM}+2G_{HM}}\right)}\right]^{-1} - \frac{G_{HM}}{6}\left(\frac{9K_{HM}+8G_{HM}}{K_{HM}+2G_{HM}}\right)$$

where K is the grain bulk modulus.

EXAMPLE

Calculate V_P and V_S in uncemented dry quartz sand of porosity 0.3 at 40 MPa overburden and 20 MPa pore pressure. Use the uncemented sand model. For pure quartz, $G = 45$ GPa, $K = 36.6$ GPa, and $\nu = 0.06$. Then, for effective pressure 20 MPa = 0.02 GPa,

$$K_{HM} = \left[\frac{9^2(1-0.36)^2 45^2}{18\cdot 3.14^2(1-0.06)^2}0.02\right]^{1/3} = 2\text{ GPa}$$

$$G_{HM} = \frac{5-4\cdot 0.06}{5(2-0.06)}\left[\frac{3\cdot 9^2(1-0.36)^2 45^2}{2\cdot 3.14^2(1-0.06)^2}0.02\right]^{1/3} = 3\text{ GPa}$$

Next,

$$K_{eff} = \left(\frac{0.3/0.36}{2+\frac{4}{3}3} + \frac{1-0.3/0.36}{36.6+\frac{4}{3}3}\right)^{-1} - \frac{4}{3}3 = 3\text{ GPa}$$

$$G_{eff} = \left(\frac{0.3/0.36}{3+0.29} + \frac{1-0.3/0.36}{45+0.29}\right)^{-1} - 0.29 = 3.6\text{ GPa}$$

Pure quartz density is 2.65 g/cm^3; then, the sandstone's density is

$$2.65\cdot(1-0.3) = 1.855\text{ g/cm}^3$$

The P-wave velocity is

$$V_P = \sqrt{\frac{3+\frac{4}{3}3.6}{1.855}} = 2.05\text{ km/s}$$

and the S-wave velocity is

$$V_S = \sqrt{\frac{3.6}{1.855}} = 1.39\text{ km/s}$$

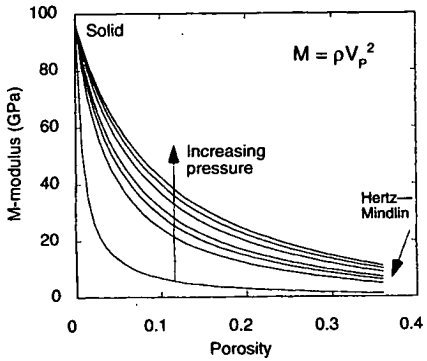

Figure 5.2.5. Illustration of the modified lower Hashin–Shtrikman bound for various effective pressures. The pressure dependence follows from the Hertz–Mindlin theory incorporated into the right end member.

This model connects two end members; one has zero porosity and the modulus of the solid phase and the other has high porosity and a pressure-dependent modulus as given by the Hertz–Mindlin theory. This contact theory allows one to describe the noticeable pressure dependence normally observed in sands.

The high-porosity end member does not necessarily have to be calculated from the Hertz–Mindlin theory. The end member can be measured experimentally on high-porosity sands from a given reservoir. Then, to estimate the moduli of sands

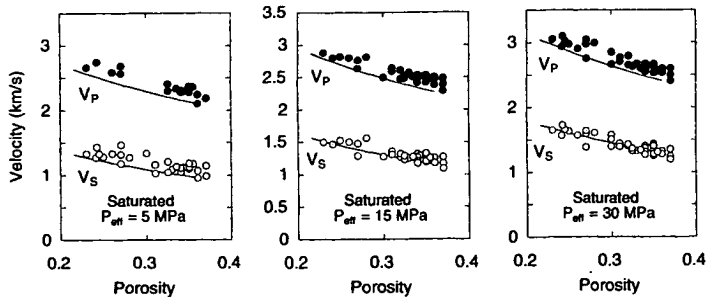

Figure 5.2.6. Prediction of V_P and V_S using the lower Hashin–Shtrikman bound compared with measured velocities from unconsolidated North Sea samples.

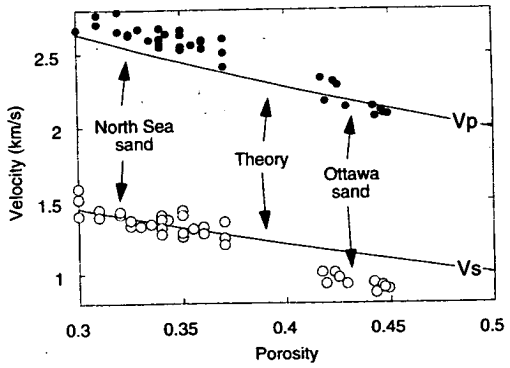

Figure 5.2.7

of different porosities, the modified Hashin–Strikman lower bound formulas can be used, where K_{HM} and G_{HM} are set at the measured values.

This method provides accurate estimates for velocities in uncemented sands. In Figures 5.2.6 and 5.2.7 the curves are from the theory.

This method can also be used for estimating velocities in sands of porosities exceeding 0.36.

USES

The methods can be used to model granular high-porosity rocks.

ASSUMPTIONS AND LIMITATIONS

The grain contact models presuppose the following:

- The strains are small.
- Identical homogeneous, isotropic, elastic spherical grains are assumed.

EXTENSIONS

To calculate the effective elastic moduli of saturated rocks (and low-frequency acoustic velocities), Gassmann's formula should be applied.

5.3 ORDERED SPHERICAL GRAIN PACKINGS – EFFECTIVE MODULI

SYNOPSIS

Ordered packings of identical spherical particles are generally anisotropic. Their effective elastic properties can be thus described through stiffness matrices.

SIMPLE CUBIC PACKING

The coordination number is 6, and the porosity is 47 percent. The stiffness matrix is

$$\begin{pmatrix} C_{11} & C_{12} & C_{12} & 0 & 0 & 0 \\ C_{12} & C_{11} & C_{12} & 0 & 0 & 0 \\ C_{12} & C_{12} & C_{11} & 0 & 0 & 0 \\ 0 & 0 & 0 & \frac{1}{2}(C_{11}-C_{12}) & 0 & 0 \\ 0 & 0 & 0 & 0 & \frac{1}{2}(C_{11}-C_{12}) & 0 \\ 0 & 0 & 0 & 0 & 0 & \frac{1}{2}(C_{11}-C_{12}) \end{pmatrix}$$

where

$$c_{11} = c_0, \quad c_{12} = \frac{\nu}{2(2-\nu)}c_0, \quad c_0 = \left[\frac{3G^2P}{2(1-\nu)^2}\right]^{1/3}$$

P is the hydrostatic pressure, and G and ν are the grain material shear modulus and Poisson's ratio, respectively.

HEXAGONAL CLOSE PACKING

The coordination number is 12, and the porosity is about 26 percent. The stiffness matrix is

$$\begin{pmatrix} C_{11} & C_{12} & C_{13} & 0 & 0 & 0 \\ C_{12} & C_{11} & C_{13} & 0 & 0 & 0 \\ C_{13} & C_{13} & C_{33} & 0 & 0 & 0 \\ 0 & 0 & 0 & C_{44} & 0 & 0 \\ 0 & 0 & 0 & 0 & C_{44} & 0 \\ 0 & 0 & 0 & 0 & 0 & C_{66} \end{pmatrix}$$

where

$$c_{11} = \frac{1152 - 1848\nu + 725\nu^2}{24(2-\nu)(12-11\nu)}c_0$$

$$c_{12} = \frac{\nu(120 - 109\nu)}{24(2-\nu)(12-11\nu)}c_0$$

$$c_{13} = \frac{\nu}{3(2-\nu)}c_0$$

$$c_{33} = \frac{4(3-2\nu)}{3(2-\nu)}c_0$$

$$c_{44} = c_{55} = \frac{6-5\nu}{4(2-\nu)}c_0$$

$$c_{66} = \frac{576 - 948\nu + 417\nu^2}{24(2-\nu)(12-11\nu)}c_0$$

FACE-CENTERED CUBIC PACKING

The coordination number is 6, and the porosity is about 47 percent. The stiffness matrix is

$$\begin{pmatrix} C_{11} & C_{12} & C_{12} & 0 & 0 & 0 \\ C_{12} & C_{11} & C_{12} & 0 & 0 & 0 \\ C_{12} & C_{12} & C_{11} & 0 & 0 & 0 \\ 0 & 0 & 0 & C_{44} & 0 & 0 \\ 0 & 0 & 0 & 0 & C_{44} & 0 \\ 0 & 0 & 0 & 0 & 0 & C_{44} \end{pmatrix}$$

where

$$c_{11} = 2c_{44} = \frac{4-3\nu}{2-\nu}c_0$$

$$c_{12} = \frac{\nu}{2(2-\nu)}c_0$$

USES

The results of this section are sometimes used to estimate the elastic properties of granular materials.

ASSUMPTIONS AND LIMITATIONS

These models assume identical elastic spherical particles under small strain conditions.